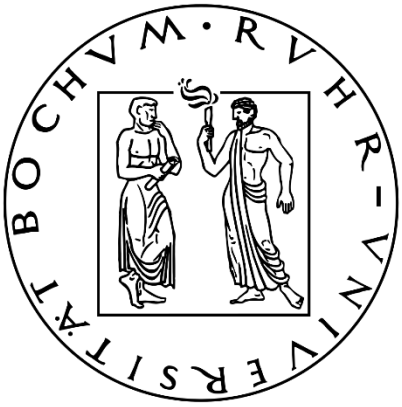

BACHELORARBEIT

vorgelegt zur Erlangung des Grades Bachelor of Science
an der Fakultät für Biologie und Biotechnologie
der Ruhr-Universität Bochum

Energietransfer über Nahrungsnetze in Untereis-Habitaten des Arktischen Ozeans

Food-Web energy transfer in under-ice habitats of the Arctic Ocean

von

APASIRI KLASMEIER

angefertigt im Alfred-Wegener-Institut,
Helmholtz-Zentrum für Polar- und Meeresforschung in Bremerhaven

Bochum, im September 2019

Betreuer*in: Dr. Hauke Flores
Erstgutachter*in: Prof. Dr. Ralph Tollrian
Zweitgutachter*in: Prof. Dr. Stefan Herlitze

ALFRED-WEGENER-INSTITUT
HELMHOLTZ-ZENTRUM FÜR POLAR- UND MEERESFORSCHUNG

RUHR UNIVERSITÄT BOCHUM
RUB

Table Of Contents

1 Abstracts

1.1 Abstract (English)

Under-ice ecosystems in the Arctic Ocean are exposed to rapid transformations in the face of climate change. Changes in oceanography and sea ice conditions will affect all trophic levels of ice-associated ("sympagic") communities. For this study, two key groups of the zooplankton community (ice-associated amphipod *Apherusa glacialis* and calanoid copepods) North of Spitsbergen were observed during summer. The research area comprised stations on the Barents Sea shelf, in the Nansen Basin and close to the Yermak Plateau.

Samples were taken at the ice-water interface layer with a Surface and Under-Ice Trawl (SUIT) and abundance, biomass and stable $\delta\ ^{13}C$ and $\delta\ ^{15}N$ isotope contents were measured. To further investigate the relation between zooplankton and higher trophic levels in this area, stomach contents of Arctic key species polar cod (*Boreogadus saida*) were examined.

The abundances of both groups showed differing patterns, pointing to higher abundances of *A. glacialis* around the Barents Sea shelf slope and higher copepod abundances in the Nansen Basin and near the Yermak Plateau. Biomasses and stable isotope contents were significantly influenced by inflow of Atlantic Water and possibly also by the origin of sea ice floes. Stomach content results were contrary to the results of previous papers, showing a larger proportion of copepods than amphipods. The results of this study contribute to a higher data resolution for Arctic marine environments and will help to monitor the occurring fast-paced changes in under-ice habitats.

1.2 Zusammenfassung (Deutsch)

Aufgrund des Klimawandels unterliegen Untereis-Ökosysteme im Arktischen Ozean drastischen Veränderungen. Eis-assoziierte („sympagische") Lebensgemeinschaften werden auf allen trophischen Ebenen von veränderten ozeanographischen Bedingungen und Meereis-Verhältnissen betroffen sein. Im Rahmen dieser Thesis wurden zwei wichtige Gruppen der nördlich von Spitzbergen ansässigen Zooplankton-Gemeinschaften untersucht (Eis-Amphipode *Apherusa glacialis* sowie Copepoden der Gattung *Calanus*). Das

Untersuchungsgebiet erstreckte sich dabei vom Barentssee Schelf und Nansen Becken bis in die Nähe des Yermak Plateaus. Mit einem Surface and Under-Ice Trawl (SUIT) wurde die Unterseite des Meereises beprobt und Abundanz, Biomasse und der Gehalt an stabilen $\delta\ ^{13}C$ und $\delta\ ^{15}N$ Isotopen der beiden untersuchten Gruppen gemessen. Außerdem wurden Mageninhaltsanalysen der Schlüsselart Polardorsch (*Boreogadus saida*) durchgeführt, um die Verbindungen zwischen höheren trophischen Ebenen und Zooplankton in diesem Gebiet zu untersuchen.

Die Abundanzen beider Gruppen zeigten unterschiedliche Muster: während *A. glacialis* häufiger in der Nähe des Barentssee Schelf-Abhangs vorzufinden war, erwies sich die Abundanz der Copepoden im Nansen Becken und nahe des Yermak Plateaus als höher. Die ermittelten Biomassen und der Gehalt an stabilen Isotopen wurden signifikant durch den Einstrom atlantischer Wassermassen beeinflusst. Weiterhin deuten die Ergebnisse auf einen Einfluss der Eisherkunft hin. Die Mageninhalte der untersuchten Polardorsche widersprechen den in bisherigen Veröffentlichungen festgestellten Verhältnissen, da ein höherer Anteil von Copepoden als Amphipoden festgestellt wurde. Die Ergebnisse dieser Thesis tragen zu einer höheren Auflösung der Datenlage mariner Ökosysteme in der Arktis und damit einer detaillierteren Überwachung der dort ablaufenden Veränderungen bei.

2 Introduction

2.1 Effects of climate change on sea ice in the Arctic Ocean

The polar regions belong to the most rapidly changing habitats in the face of global warming. In addition to threats like rising sea temperatures and ocean acidification, the aquatic communities in polar waters are confronted with the continued reduction of sea ice (Comiso, 2003; Vaughan *et al.*, 2013).

The occurrence of sea ice can be measured in various ways. Most commonly it is given as sea ice extent, sea ice area or sea ice concentration (Lubin and Massom, 2006). Sea ice extent in the Arctic Ocean in the past 13 years has shown distinct deviations from the 30-year mean and is reaching another minimum in the summer of 2019, as shown in Fig.1-1 (Perovich, 2011).

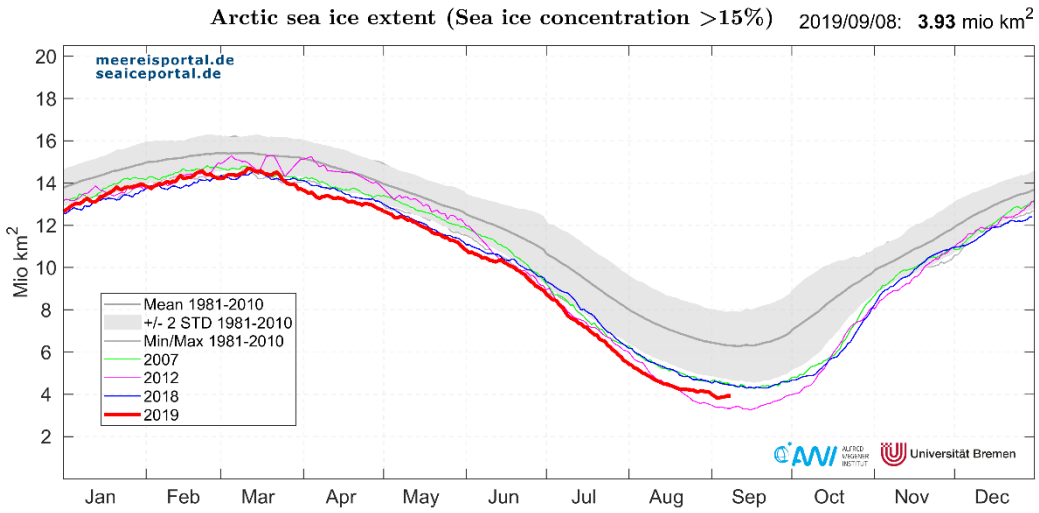

Fig. 1-1. Sea ice extent (mio. km²) in the Arctic Ocean as of 8th September 2019. (Spreen, Kaleschke and Heygster, 2008; Grosfeld *et al.*, 2016).

A summer sea ice extent of less than one million km² in the Arctic Ocean would be considered an "ice-free" summer (Wang and Overland, 2009). Predictions of when the first ice-free summer will occur are still uncertain, but in the face of rising global temperatures the occurrence of the phenomenon itself is expected in the course of the 21st century (Wang and Overland, 2009, 2012). The ecological consequences of an ice-free Arctic Ocean are being investigated in numerous polar research papers.

2.2 Under-ice habitats

Sea ice plays an important role as an abiotic factor in aquatic polar ecosystems (Ackley and Sullivan, 1994; Cottier, Steele and Nilsen, 2017; Thomas, 2017). For a variety of primary producers, such as algae and phytoplankton, sea ice and especially the under-ice zone serve as a habitat. Zooplanktonic herbivores and their associated predators are therefore likewise dependent on sea ice, not only for foraging, but also for protection from higher predators (David *et al.*, 2015; Flores and Macke, 2018; Schaafsma, 2018). Due to climate change the available under-ice habitat is decreasing. It is therefore essential to observe the changes in these specific ecosystems to calculate their consequences for population structures, species diversity and food chains in the polar regions as a whole (Werner and Gradinger, 2002; Berge *et al.*, 2012; Kohlbach *et al.*, 2016, 2018; Kohlbach, Lange, *et al.*, 2017; Kohlbach, Schaafsma, *et al.*, 2017; Schaafsma, 2018; Flores *et al.*, 2019).

2.3 Ice-amphipod *Apherusa glacialis*

Amphipods belong to the dominant animal taxa in sea-ice ecosystems (Bradstreet and Cross, 1982; Berge *et al.*, 2012). One of the most numerous ice-associated amphipod species is *Apherusa glacialis* (Hansen, 1888), found at the underside of the sea ice (Werner and Gradinger, 2002; Werner and Auel, 2005; Arndt and Swadling, 2006; Berge *et al.*, 2012; David *et al.*, 2015). Large female animals can reach a size of more than 17 mm (Poltermann, Hop and Falk-Petersen, 2000) and a lifespan of up to 2 years (Beuchel and Lønne, 2002). Reproduction occurs in winter (Berge *et al.*, 2012) and juvenile animals are released from the brood pouches of females over a longer period of time, mostly in March (Poltermann, Hop and Falk-Petersen, 2000). *Apherusa glacialis* has been described as both strictly herbivorous (Werner and Auel, 2005) and mainly detritivorous (Poltermann, 2001). According to (Bradstreet and Cross, 1982) and more recent papers (Arndt and Swadling, 2006; Kohlbach *et al.*, 2016), it is feeding primarily on ice microalgae. For polar cod, amphipods present one of the main food sources in under-ice ecosystems (Bradstreet and Cross, 1982; Kohlbach, Schaafsma, *et al.*, 2017). Amphipods therefore form an important trophic link between primary producers and higher trophic levels such as seabirds and marine mammals that prey on fish (Bradstreet and Cross, 1982; Gulliksen and Lønne, 1989).

2.4 Calanoid copepods *Calanus hyperboreus*, *Calanus glacialis* and *Calanus finmarchicus*

A major proportion of marine zooplankton biomass in the Arctic Ocean and sub-arctic Atlantic consists of calanoid copepods such as *Calanus finmarchicus* (Gunnerus, 1765), *Calanus glacialis* (Jaschnov, 1955) and *Calanus hyperboreus* (Kroyer, 1838) (Kosobokova and Hirche, 2009). They therefore provide an important link between primary producers and higher trophic levels (Klekowski and Weslawski, 1991). While *C. finmarchicus* typically occurs in the North Atlantic, *C. glacialis* and *C. hyperboreus* are commonly found in the Arctic Ocean. *C. glacialis* is usually associated with Arctic shelf regions and *C. hyperboreus* with deep-water areas (Conover, 1988; Falk-Petersen *et al.*, 2009). Recent research indicates that the commonly assumed geographical distribution of the three species could be broader and more overlapping than previously thought, since their distinction on morphological grounds is debated (Choquet *et al.*, 2017). Usually, the morphologically very similar *C. finmarchicus* and *C. glacialis* are differentiated by measurement of their prosome length (Hirche *et al.*, 1994; Daase *et al.*, 2018). Likewise, the developmental stages of calanoid copepods can be distinguished morphologically (Hirche and Kwasniewski, 1997). Developmental stages are structured in nauplius larvae, copepodite stages CI-CV and adulthood (Kosobokova, 1999). The regular lifecycle of *Calanus* species is spatio-temporally structured in three distinct phases. The main developmental and growth phase is performed during spring and summer. In winter, the copepods retreat to deeper waters and reduce their metabolism (Falk-Petersen *et al.*, 2009). The final developmental stages are reached around autumn or spring. The lifespans and lifecycle durations vary between the three species. While *C. finmarchicus* was shown to have a lifecycle of one year, *C. glacialis* often has a two-year lifecycle and *C. hyperboreus* was shown to regionally reach a lifespan of up to 4-6 years (Falk-Petersen *et al.*, 2009).

.

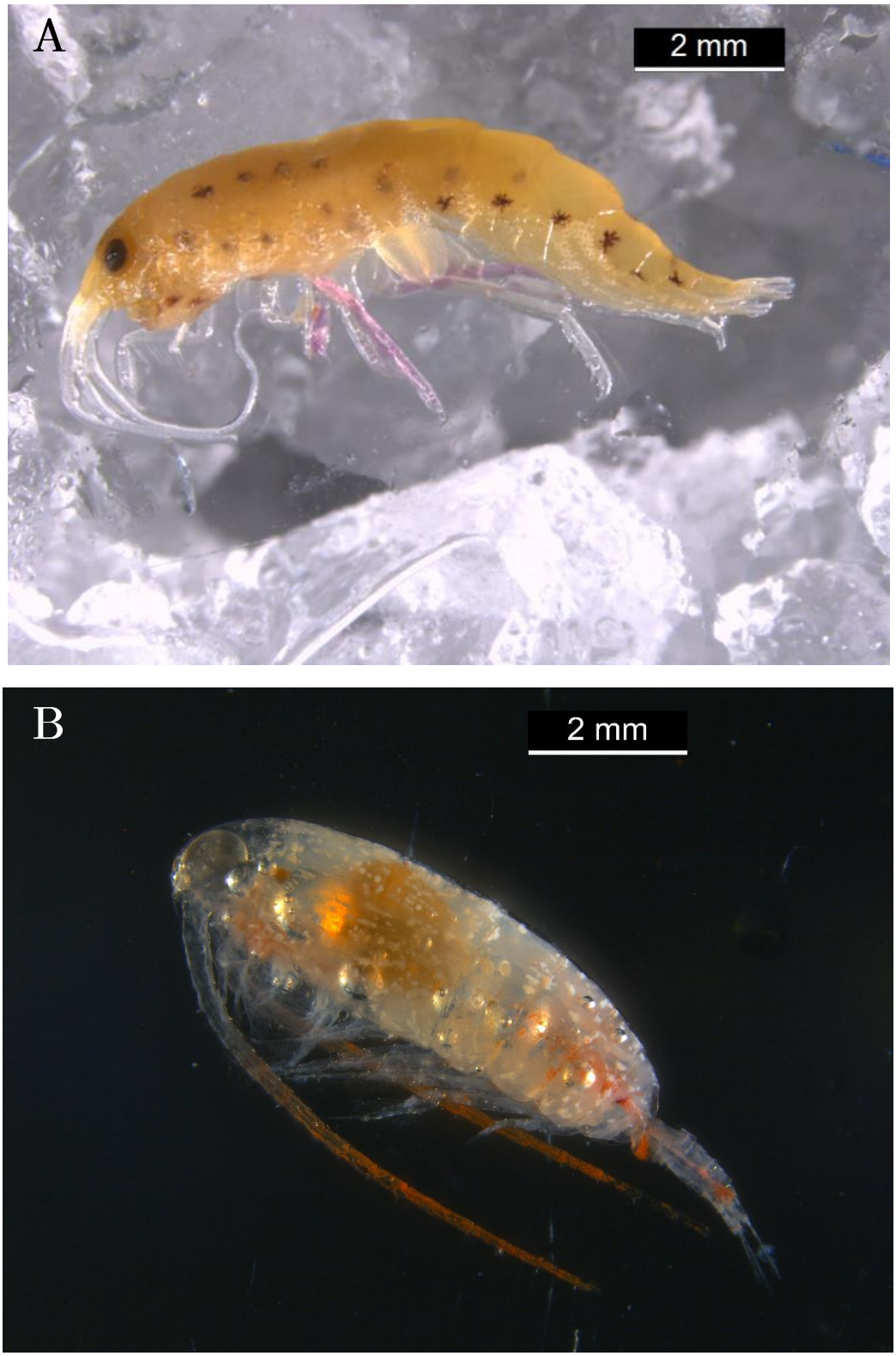

Fig. 1-2. (A) Ice-amphipod *Apherusa glacialis*, (B) *Calanus hyperboreus* female.

2.5 Polar cod *Boreogadus saida*

The most abundant fish species residing under the pack-ice in the Arctic Ocean is polar cod *Boreogadus saida* (Lepechin, 1774) (Gulliksen and Lønne, 1989; Hop and Gjøsæter, 2013; David *et al.*, 2016). Mostly young polar cod (aged 1 or 2 years) find refuge in under-ice habitats, while older and sexually mature specimens retreat to pelagic zones and are therefore rare under the ice (Gulliksen and Lønne, 1989). Young polar cod caught under the ice were described to reach a body size of up to 168 mm (Lønne and Gulliksen, 1989). Polar cod were shown to play a major role in transfer of energy from lower to higher trophic levels (Bradstreet and Cross, 1982). The diet of *B. saida* is dominated by copepods and ice-associated amphipods (Bradstreet and Cross, 1982; Christiansen *et al.*, 2012; Kohlbach, Schaafsma, *et al.*, 2017)

2.6 Aim of study and objectives

One aim of this study is to provide detailed information on the composition of under-ice communities north of Spitsbergen. Abundance, horizontal distribution and ontogenetic development of two key species of several sampling locations on shelf, slope and basin areas were investigated for this purpose. Furthermore, the study aims to investigate trophic links in under-ice ecosystems that were detected in previous research. Two exemplary methods (stable isotope analysis and stomach content analysis) were used to illustrate links between zooplankton and primary producers as well as predatory fish.

2.7 Hypotheses

a) If under-ice habitats are located over different depth levels (e.g. shelf or basin) and below sea ice floes of different origin sectors, then zooplankton abundance and stable isotope proportion will show distinct spatial variabilities.

b) Following hypothesis a), if young polar cod are found in these under-ice habitats, the availability and quality of their food resources will differ.

3 Methods

3.1 Cruise PS106

All analyzed samples were taken during expedition PS106 of the research vessel POLARSTERN to the waters north and east of Spitsbergen in 2017. Sampling was conducted on cruise leg 2 (23 June 2017 - 20 July 2017) between Longyearbyen and Tromsø. Samples of 16 stations were taken into account for this thesis. Starting at station 50-5 on the Barents Sea shelf over a relatively shallow area of 102 m depth, the research vessel moved northwards into the Nansen Basin over a maximum depth of 4051 m at station 74-5. Turning southwards, the vessel headed towards the slope of the Yermak Plateau into the Sofia Basin. The last station 79-1 was located in an area with a depth of 2849 m. Station metadata and an overview of sampling locations are depicted in Table 1 and Fig. 2-1. The sea ice concentrations around Spitsbergen at beginning and end of the cruise are shown in Fig. 2-2. Detailed information on expedition PS106 can be found in the respective cruise report (Flores and Macke, 2018).

Table 1. List of sample stations

Station	Date	Time (UTC)	Latitude	Longitude	Depth (m)	Net
PS106_50-5	29.06.2017	07:12	80.54684	31.2413	102	PLK
PS106_63-1	01.07.2017	12:23	81.45766	32.8147	223	PLK
PS106_65-4	02.07.2017	06:25	81.58989	33.23903	519	PLK
PS106_66-4	02.07.2017	15:44	81.66362	32.32066	1591	PLK
PS106_67-5	03.07.2017	18:25	81.95776	32.48194	2786	Shrimp
PS106_68-5	04.07.2017	10:36	82.3369	33.02589	3009	PLK
PS106_69-2	05.07.2017	08:09	82.99359	33.17986	3718	PLK
PS106_70-1	05.07.2017	17:18	83.1104	32.80092	3808	PLK
PS106_71-5	06.07.2017	06:41	83.30934	33.20761	3885	PLK
PS106_72-5	06.07.2017	15:27	83.49164	33.11674	3980	PLK
PS106_73-7	07.07.2017	08:47	83.68356	32.05169	4023	Shrimp
PS106_74-5	08.07.2017	13:14	83.47596	27.90758	4051	PLK
PS106_75-6	09.07.2017	11:05	82.99111	25.27466	4048	PLK
PS106_77-2	10.07.2017	15:46	82.25277	17.85313	2008	PLK
PS106_78-5	11.07.2017	06:49	82.05883	17.79218	3169	PLK
PS106_79-1	11.07.2017	17:11	81.66446	17.02542	2849	PLK

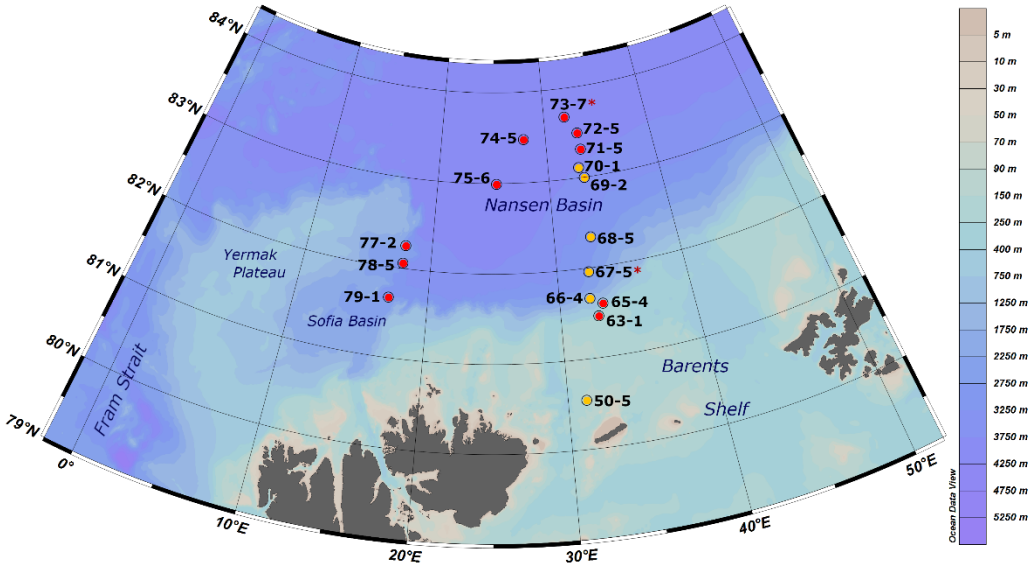

Fig.2-1. Station map based on Table 1. Samples of stations 67-5 and 73-7 from shrimp net (marked with red asterisks), all other samples from PLK net. (Red dot = samples were scanned for *Calanus* spp., *Calanus hyperboreus* and *Apherusa glacialis*; yellow dot = samples were only scanned for *Apherusa glacialis*).

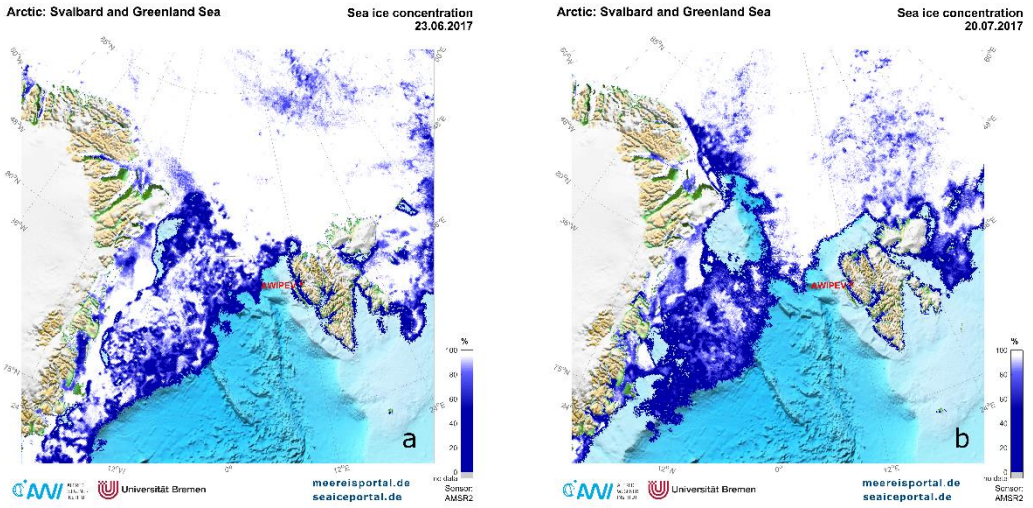

Fig. 2-2. Sea ice concentration at (a) beginning and (b) end of cruise PS106.2. Data provided by Thomas Krumpen, AWI using a sea-ice back-tracking algorithm following (Spreen, Kaleschke and Heygster, 2008; Grosfeld *et al.*, 2016).

3.2 Surface layer sampling

The samples considered in this thesis were taken exclusively in ice-covered areas. The uppermost 2 m of the ice-covered waters were scoured horizontally with a Surface and Under-Ice Trawl (SUIT) (Franeker, Flores and Dorssen, 2009). The SUIT's construction is based on a 2 m x 2 m steel frame. Attached to the frame are two nets, a commercial shrimp net and a mesozooplankton net (PLK) with a length of 15 m each. The shrimp net with a mesh size of 7 mm and a width of 1.5 m was used for catching mesozooplankton as well as young polar cod (*Boreogadus saida*). The zooplankton net (PLK) with a mesh size of 0.15 mm and a width of 0.5 m was used for catching mainly zooplankton. After deployment, the SUIT was towed besides the vessel for a duration of approximately 0.5 hours, covering a distance of at least 825 m and up to 2875 m per Station. For this thesis, mainly mesozooplankton samples caught with the PLK were taken into account, except for stations 67-5 and 73-7 due to complications with the PLK net during sampling. After collection, zooplankton samples were preserved on 4 % formaldehyde-seawater solution and stored at room temperature or frozen at -20 °C or -80 °C, and taken to the Alfred-Wegener-Institute in Bremerhaven. Polar cod were either frozen whole at -20 °C or dissected, and the stomachs preserved on 4 % formaldehyde as well. For further information on construction and application of the SUIT on this expedition, consider (Flores *et al.*, 2012; David *et al.*, 2015; Flores and Macke, 2018).

3.3 Species abundance and horizontal distribution

The use of protective nitril gloves and working under a fume hood were required during the whole examination process. Before examination, each sample was placed in a sieve and rinsed with tap water for at least 10 min to wash away the formaldehyde. After rinsing, the samples were split using a Motoda zooplankton splitter (Motoda, 1959). In subsamples of 0.015 to 0.475 of the total sample, the abundances of four zooplankton species were counted using a Leica M205 C microscope and a Bogorov counting chamber. 16 stations were scanned for amphipod species *Apherusa glacialis*. Abundances and photos of *A. glacialis* at five of the 16 stations (50-5, 66-4, 67-5, 68-5, 70-1) and for subsamples of four stations (63-1, 65-5, 77-1, 78-5) were provided by Nadine Knüppel, AWI. 10 of the 16 stations were furthermore investigated for the three copepod species *Calanus hyperboreus*, *Calanus finmarchicus* and *Calanus glacialis*. Copepod individuals were counted and

if possible assigned to their respective ontogenetic stages (ranging from CII-III, CIV and CV to adult females) as depicted in the "Atlas of the Marine Fauna of Southern Spitzbergen" (Klekowski & Weslawski, 1991). The prosome length of *C. finmarchicus* and *C. glacialis* typically ranges from ≤3.1 to 4.4 mm in the adult stages. Both species look very similar and are commonly differentiated morphologically based on their prosome length (Unstad and Tande, 1991; Hirche *et al.*, 1994; Kwasniewski *et al.*, 2003; Arnkværn, Daase and Eiane, 2005). The two species *C. finmarchicus* and *C. glacialis* were therefore referred to with the collective term *Calanus* spp. during the counting process and only later distinguished as described in section 4.5. The species *C. hyperboreus* usually reaches a prosome length of ≥4.5 mm in its adult stage and bears a characteristic thorn on last segment of the prosome (Klekowski and Weslawski, 1991). It is therefore more easily distinguishable from the other two *Calanus* species. The rarely occurring calanoid copepods of either species identified as ontogenetic stage CIII or lower were counted as "copepodites", and not differentiated to species level.

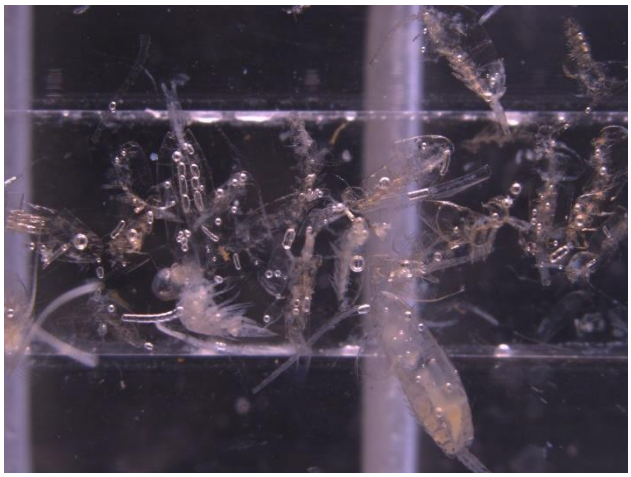

Fig. 2-3.
Sample with damaged copepods in Bogorov counting chamber.

Due to heavy physical damage of several samples, perhaps caused by loose ice entering the net during sampling, not all copepod individuals could be identified down to ontogenetic stage or species level (see Fig.2-3). Damaged and thus unidentifiable calanoid copepods were listed as "damaged individuals". Remains of urosomes were counted as equal to one damaged individual, since they were more robust than prosomes. Remains of prosomes were therefore not taken into account. The majority of the damaged individuals were assumed to belong to ontogenetic stage CIV or higher (assumptions

based on prosome length and/or number of urosome segments). Following the examination, all specimens were fixated in 70 % ethanol or 4 % formaldehyde.

3.4 Photographic documentation and length measurements

After counting (see 4.3), photos of the specimens were taken using the Leica M205 C microscope and the program Leica Application Suite (LAS) version 4.12.0. Detailed information on microscope and camera equipment are listed in Table 6 (see appendix). Individuals in a good condition of each ontogenetic stage and each species were photographed. The length of the photographed specimens was then measured in mm. *Calanus* spp. and *Calanus hyperboreus* were measured from tip of the head to end of the prosome, *Apherusa glacialis* was measured from tip of the head to end of the telson (as shown in fig x). Frozen samples were cooled with ice during the whole process.

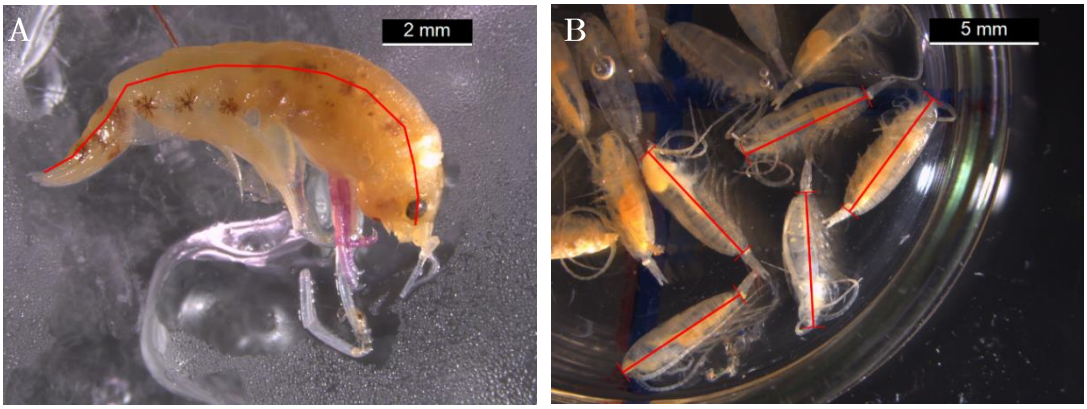

Fig. 2-4. Examples of length measurements of (A) *Apherusa glacialis* and (B) *Calanus* spp.

3.5 Calculation of biomass

For the calculation of the biomass of *Apherusa glacialis* at each station, not only formaldehyde samples but also frozen samples from the same stations and nets were taken into account (see Table 5). The preparation of frozen samples is described in section 3.6. Photographic documentation of the prepared samples was performed following the same guidelines as the formaldehyde samples.

Based on the length and weight data of frozen *A. glacialis* samples, a length-weight-regression as shown in Fig. 2-5 was prepared by N. Zakharova (Zakharova, 2019). The resulting Equation (1) could then be used for calculation of the mean dry weight (mg) of the individuals in the formaldehyde samples analyzed in section 3.3, inserting the total mean length (mm) of 7.5 mm for *A. glacialis* in formaldehyde samples as $\bar{x}$. The dry weight in mg per m^2 for each station was calculated following Equation (2), multiplying the mean dry weight (mg) with the abundances (Ind m^{-2}) of *A. glacialis* at each station.

$$mean\ DW_{[mg]} = 0.013892 * \bar{x}^{\,2.439700} \tag{1}$$

$$DW_{[mg\ m^{-2}]} = mean\ DW_{[mg]} \cdot abundance_{[\frac{ind}{m^2}]} \tag{2}$$

For the calculation of copepod biomasses, the abundance (Ind m^{-2}) calculated in section 3.3 was converted into dry weight (mg Ind^{-1}), using dry weight reference values obtained from the literature. For *C. glacialis* and *C. hyperboreus* stages CIV, CV and Female, biomasses were converted referring to the mean carbon (µg Ind^{-1}) and mean carbon content (prop. dry weight) as given in (Ashjian *et al.*, 2003), following Equation (3). Reference dry weight values used in (Richter, 1994) were applied for *C. finmarchicus* stages CIV, CV and Females as well as copepodites (reference value for stage CIII) and damaged individuals (reference value for stage CV). The copepod biomasses were calculated in the same way as *A. glacialis* biomasses, following Equation (2).

$$mean\ DW_{[mg\ Ind^{-1}]} = 0.001 * \frac{mean\ carbon_{[\mu g\ Ind^{-1}]}}{mean\ carbon\ content_{[prop.\ \ dry\ wt]}} \tag{3}$$

All biomasses were expressed as dry weight in mg per m^2.

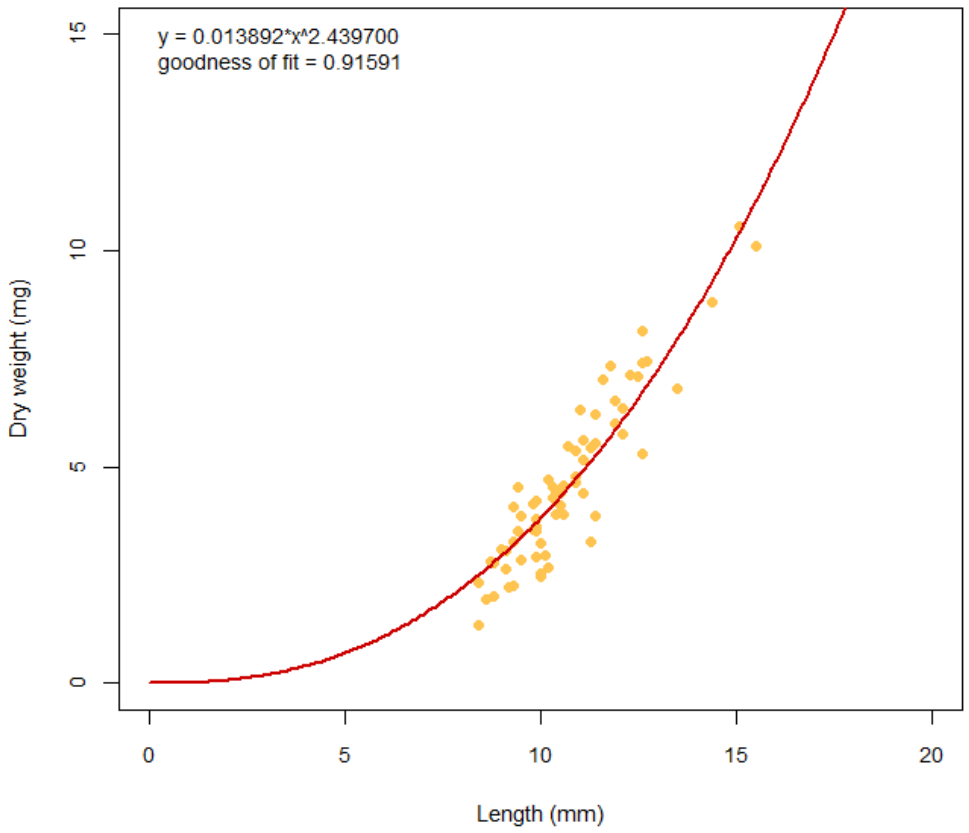

Fig. 2-5. Length-weight-regression of *Apherusa glacialis* frozen samples. (n=70; modified after (Zakharova, 2019))

3.6 Bulk Stable Isotope Analysis (BSIA)

For bulk stable isotope analysis, frozen SUIT samples of the same stations and hauls stored at -20 ˚C were used. 21 *Apherusa glacialis* individuals caught at 10 stations and 15 *Calanus* spp. individuals from one station were taken into account (see appendix, Table 5).

The samples were defrosted in a 2 °C fridge and dabbed with KimWipes to remove excess water. They were then photographed and their lengths measured as described in section 3.5. Subsequently, the samples were put into 1.5 ml glass vials and freeze-dried for 24 h at a chamber pressure of 0.133 mbar using a Zirbus Technology Sublimator VaCo5. The dried samples were stored in desiccators. Weight measurements of the dried samples were performed using a Mettler Toledo UMX-2 fine scale. Tweezers and spatulas were deionized using a Mettler Toledo EN SL LC Deionizer. The samples were taken out of the vials individually and put on a square cut of

aluminum foil during weight measurement. After a fixed waiting period of 10 seconds, the weight in mg was noted. Extensive waiting periods are not recommended, since the samples will take up humidity from the air and increase in weight. After weighing, samples were homogenized mechanically and individually using a mortar and afterwards loaded into 5x9 mm tin capsules for solids. The tin capsules were folded into spherical shape following the Littoral Environnement et Sociétés Stable Isotope Facility (LIENSs SIF) protocol for sample preparation (LIENs Stable Isotope Facility, 2014). The spheres were placed in a sealed well plate and sent to LIENs SIF, La Rochelle, for bulk stable isotope analysis. All samples were analyzed with a continuous flow isotope ratio mass spectrometer Delta V Plus, interfaced with an elemental analyzer (either Flash EA 1112 (sample 6609) or Flash 2000 (all other 35 samples)) and connected via a Conflo IV interface (Thermo Scientific Corporation, Germany). The reference materials used for calibration of the stable isotopes measurements were for d ^{13}C: USGS-24, IAEA-CH6, IAEA-600, USGS-61, USGS-62 and for d ^{15}N: IAEA-N2, IAEA-NO-3, IAEA-600, USGS-61, USGS-62. The analytical precision was <0.10 ‰ for δ ^{13}C and <0.15 ‰ for δ ^{15}N. Isotope results are expressed in the delta (δ) unit notation as deviations from standards (Vienna Pee Dee Belemnite for δ ^{13}C and N_2 in air for δ ^{15}N). More detailed information on methodology and analytical conditions are provided in (LIENs Stable Isotope Facility, 2014; Kohlbach *et al.*, 2016; Zakharova, 2019).

3.7 Stomach content analysis (*Boreogadus saida*)

Polar cod stomachs were either pre-dissected during the expedition and stored on 4 % formaldehyde, or dissected out of the whole fish for this thesis. Five fish caught with the SUIT Shrimp net at stations 50-5 and 67-5 and with the PLK net at station 70-1 were analyzed. The work on 3 polar cod samples was conducted at Wageningen Marine Research, Den Helder, Netherlands, under supervision of Dr. Fokje Schaafsma, and two fish stored at AWI were dissected at AWI. The dissected stomachs were first weighed on a Sartorius ME 235S scale. The stomachs were then emptied and weighed again. Stomach contents on formaldehyde were rinsed as described in section 3.3. under the same safety measures. The stomach contents were examined using a stereo microscope and occurrences of all identifiable prey items were counted. The overall degree of digestion of stomach contents was classified from 1 (good condition - fresh, no signs of digestion) to 4 (heavily digested - no body structures or eyes visible), similar to (Kock *et al.*, 2008). Stomachs and stomach contents were preserved on 70 % ethanol after examination.

4 Results

4.1 Species abundance and horizontal distribution

The total abundances of each counted category were first plotted onto bathymetric maps using Ocean Data View (Schlitzer, 2018) for an overview of geographical distribution as seen in Fig. 3-1. The abundances in individuals per m^2 for each station were also depicted in barplots (see Fig. 3-2). Results for *Calanus spp.* and *Calanus hyperboreus* were split into ontogenetic stages. All damaged *Calanus* individuals were assigned to *Calanus* spp. due to the high abundance of this group; damaged individuals of *Calanus hyperboreus* were negligible.

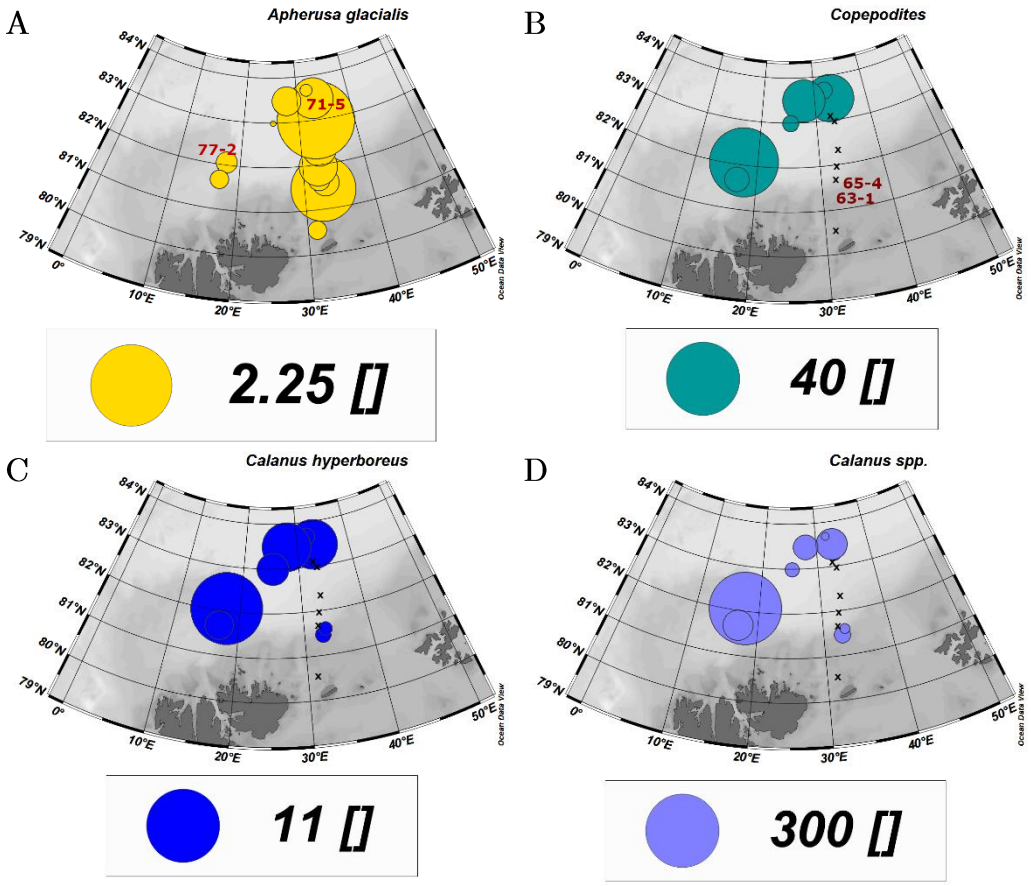

Fig. 3-1. Horizontal distribution of the abundances (individuals per m^2) of (A) *A. glacialis*, (B) copepodites, (C) *C. hyperboreus* and (D) *Calanus* spp. Black x = no data, Red station name = Abundance equals zero. Number of stations: n(Apherusa)=16, n(Calanus)=10.

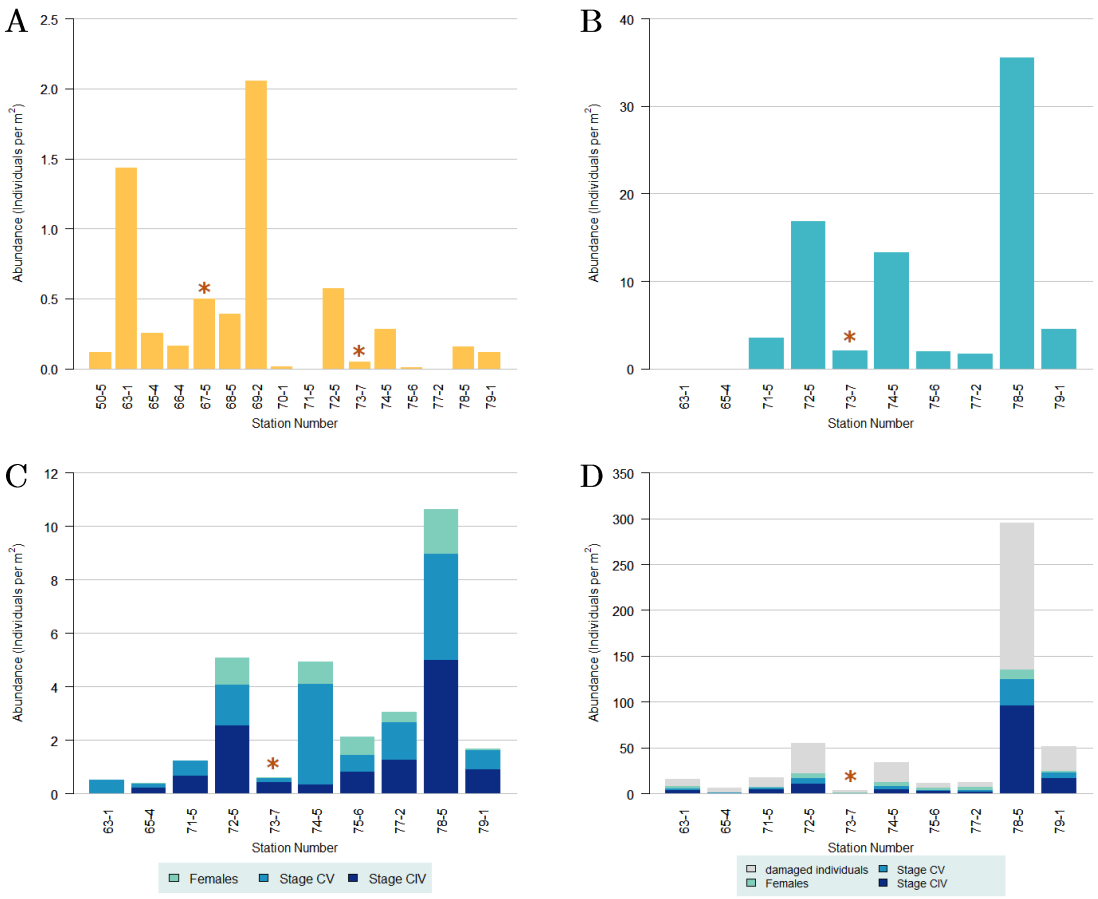

Fig. 3-2. Abundance (individuals per m²) of (A) *Apherusa glacialis,* (B) copepodites, (C) *Calanus* spp. and (C) *C. hyperboreus.* Data collected for all 16 stations in the sampling area. Samples of stations 67-5 and 73-7 from shrimp net (marked with red asterisks), all other samples from PLK net.

As shown in Fig. 3-1 and Fig. 3-2, the overall abundance of *Apherus glacialis* was higher at stations located East of 30 °E than at stations West of 30 °E. The highest abundances of 2.05 and 1.4 individuals per m² were found at station 69-2 in the Nansen Basin and station 63-1 on the shelf slope. The lowest abundances of <0.05 ind. m² were found at stations 70-1, 73-7 and 75-6 located in the Nansen Basin. At station 71-5 in the Nansen Basin and 77-2 at the slope of Yermak Plateau, the abundance of *A. glacialis* was equal to zero.

The spatial distribution of *C. hyperboreus*, *Calanus* spp. and copepodites was very similar. *C. hyperboreus* and copepodites showed a higher relative abundance at stations 72-5 and 74-5 in the North of the research area compared to station 78-5 on the slope to Yermak Plateau than *Calanus* spp.. Since there were less data points available for the stations located East of 30 °E, results for stations 50-5 as well as 66-4 to 70-1 were not comparable

between *A. glacialis* and copepods. In general, the abundances of copepod species, ranging from maximum values of up to 10.6 ind. m^2 (*C. hyperboreus*) and 35.5 ind. m^2 (copepodites) to 295.7 ind. m^2 (*Calanus* spp.), were several factors higher than abundances of *A. glacialis*. It is important to note that at most stations, more than 50 % of counted *Calanus* spp. individuals were, in fact, damaged individuals. Damaged individuals should therefore not be neglected in estimating abundance and horizontal distribution.

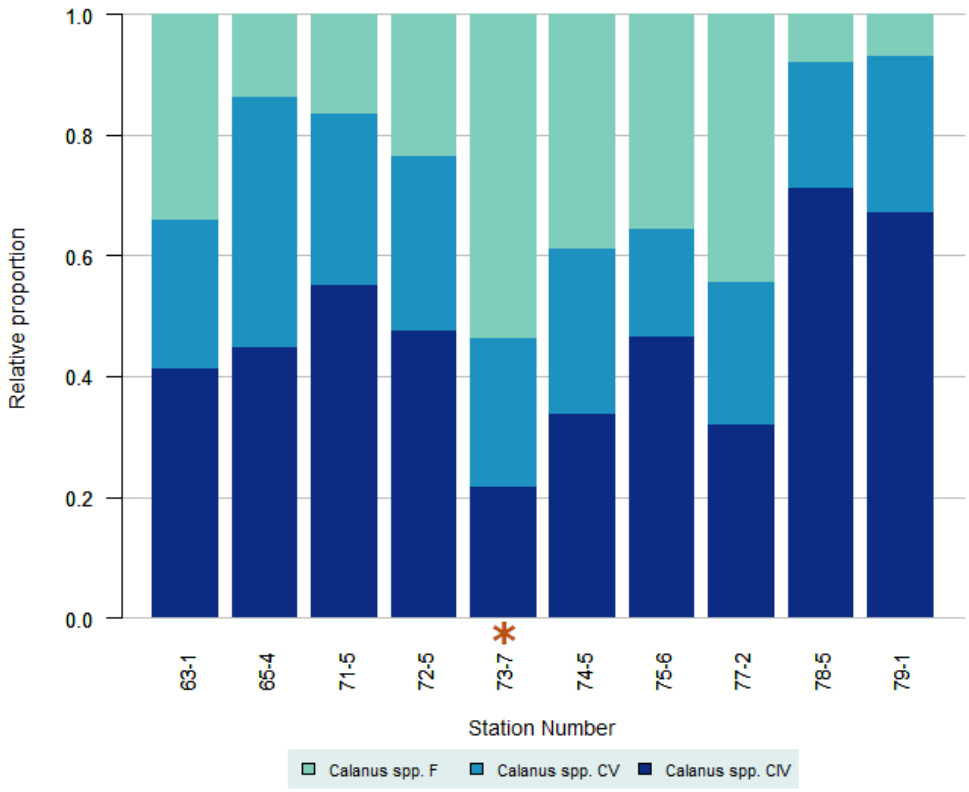

Fig. 3-3. Relative stage distribution of *Calanus* spp. stages CIV, CV and adult females per Station. Damaged individuals not included. Data collected at 10 stations in the sampling area. Sample of station 73-7 from shrimp net (marked with red asterisk), all other samples from PLK net.

As seen in Fig. 3-3, stage CIV was the most abundant of all stages when damaged individuals were not included in the stage distribution. The proportion of stage CV was around 20-30 % at all stations except 65-4, where CV proportion amounted to >40 %. All adult individuals found were female. The highest proportions of females were found in the samples

collected at stations 73-7 to 77-2 on the way from Northern Nansen Basin to the slope of Yermak Plateau. The sample examined for station 73-7 was caught with a shrimp net and not the zooplankton net and showed lower abundances of copepods than samples from the two surrounding stations.

4.2 Species differentiation of *Calanus* spp.

As described in 3.3, individuals of the species *Calanus finmarchicus* and *Calanus glacialis* have a very similar body structure and size range and can be distinguished by analyzing their size distribution. Therefore, all length measurements recorded of *Calanus* spp. individuals of the stages CIV-AF were depicted in length distribution frequency histograms shown below. No lower stage size distributions were depicted, since differences in size are most noticeable in advanced developmental stages.

Following the size references given in (Unstad and Tande, 1991; Hirche *et al.*, 1994; Kwasniewski *et al.*, 2003; Arnkværn, Daase and Eiane, 2005), the detected size distributions of all stages matched the literature values. Measured individuals were classified according to the following prosome size criteria:

Stage CIV: *C. finmarchicus* $\leq$2.1 mm$<$ *C. glacialis*
Stage CV: *C. finmarchicus* $\leq$2.9 mm$<$ *C. glacialis*
Adult Females: *C. finmarchicus* $\leq$3.1 mm$<$ *C. glacialis*

In each of the three histograms, lows can be recognized at the respective size threshold.

Following the classification, the species proportion per station and stage was calculated and visualized in Table 4 (see appendix) and Fig. 3-5. The overall proportion of *C. finmarchicus* was generally higher than the proportion of *C. glacialis*, especially regarding stages CIV and CV and taking into account that these stages showed a higher abundance at all of the stations, as described in 4.1. Only on the shelf slope stations 63-1 and 65-4, the proportion of *C. glacialis* stage CIV reached $\geq$50 %. Regarding stations 71-5 to 77-2 from Central Nansen Basin down to Yermak Plateau slope, *C. glacialis* predominated the adult female stage, reaching proportions of up to 98 % (73-7) and even 100 % at station 77-2. At the four other stations 63-1 and 65-4 on Barents Sea Shelf slope and 78-5 and 79-1 close to Yermak Plateau

slope/Sofia Basin, females of *C. finmarchicus* prevailed with proportions between 67-82 %.

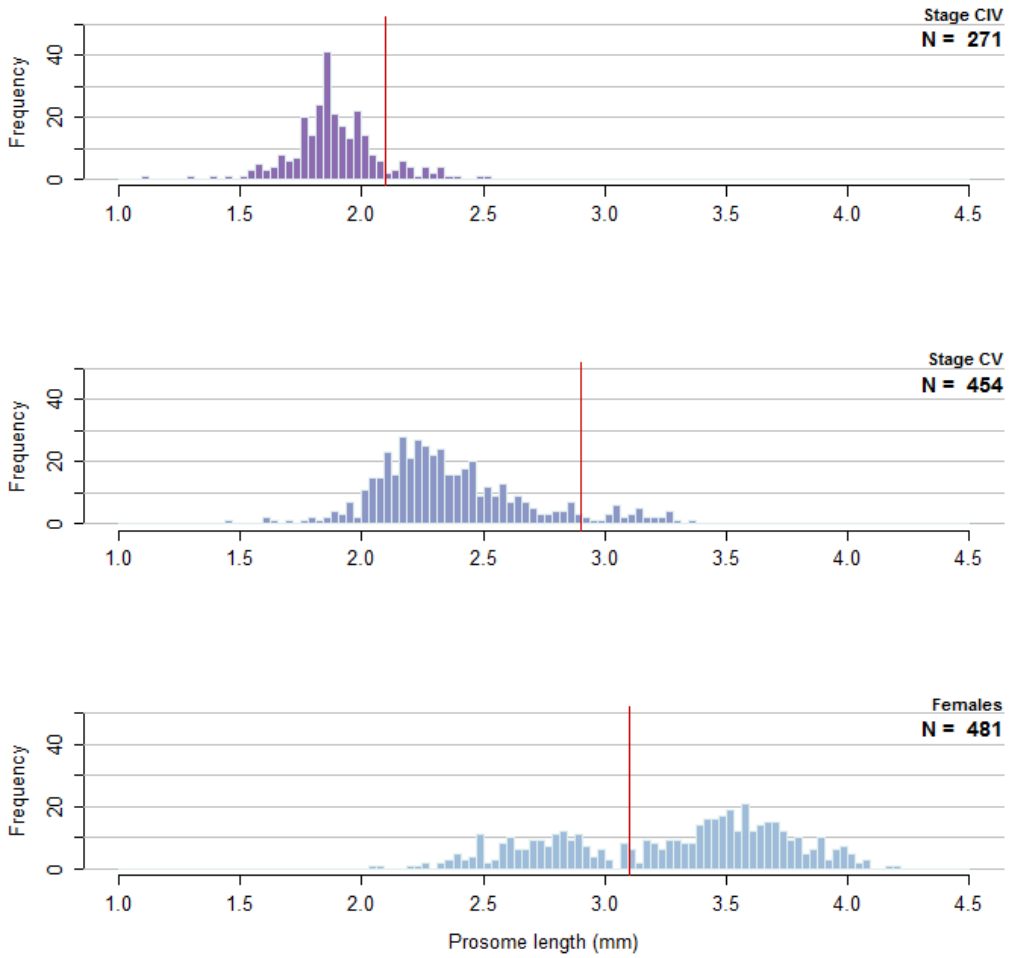

Fig. 3-4. Length distribution of *Calanus* spp. stage CIV, CV and female prosome lengths. Size thresholds for the species differentiation of *C. finmarchicus* and *C. glacialis* per stage marked as red vertical line. Data collected at 10 stations in the sampling area.

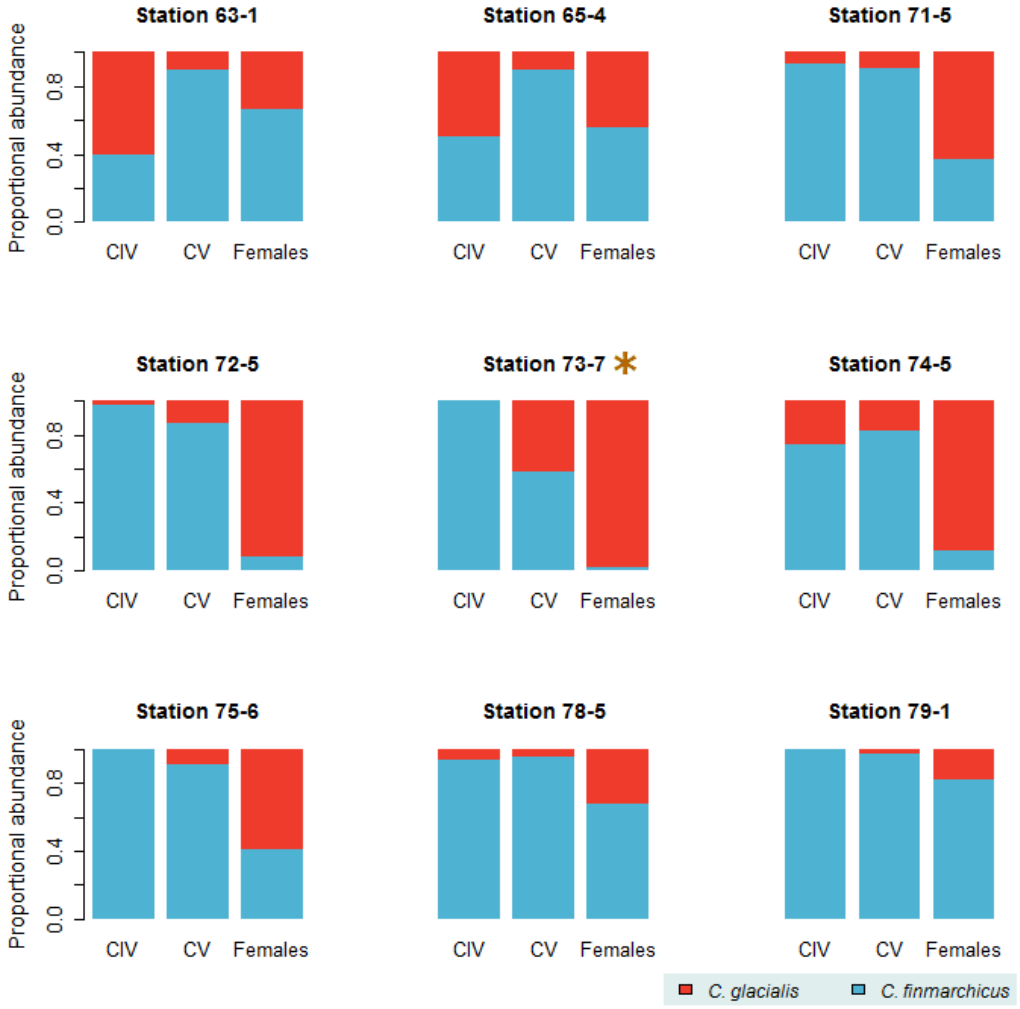

Fig. 3-5. Relative proportion of the species *Calanus finmarchicus* and *Calanus glacialis* per station and stage. Sample of station 73-7 from shrimp net (marked with red asterisk), all other samples from PLK net. Station 77-2 not shown in this plot, since data not available for stages CIV and CV. See Table 4 in the appendix.

4.3 Biomass

The dry weights (mg m^{-2}) of both *Apherusa glacialis* and calanoid copepods were plotted in a stripchart with highlighted median values as seen in Fig. 3-6 to show a comparison in biomass. Since lower copepod abundances were detected at station 73-7 where the shrimp net was used, the station was excluded from copepod biomass calculations. It was suspected that smaller individuals were not caught due to the bigger mesh size and low abundance numbers were therefore artificial. The effects of the shrimp net on abundance numbers of *A. glacialis* were assumed to be

negligible, since this species reaches a larger body size. Despite the occurence of large individuals and a resulting mean body length of 7.5 mm, the biomasses of *A. glacialis* with a median of 0.3 mg m^{-2} were the lowest of all compared species due to the low abundances described in 4.1. The biomass values of the largest copepod species *C. hyperboreus* with a median value of 4.25 mg m^{-2} were considerably higher than of *C. finmarchicus* (median: 1.28 mg m^{-2}) and *C. glacialis* (median: 1.42 mg m^{-2}), despite lower abundances. Damaged individuals showed the highest outlier of up to 43.9 mg m^{-2} (at Station 78-5) compared to the other copepod groups, but a lower median value (2.65 mg m^{-2}) than *C. hyperboreus*. When adding up the biomasses of all three *Calanus* species, copepodites and damaged individuals, depicted as *Calanus* spp., the median value increased to 8.9 mg m^{-2} and the highest outlier reached 87 mg m^{-2}.

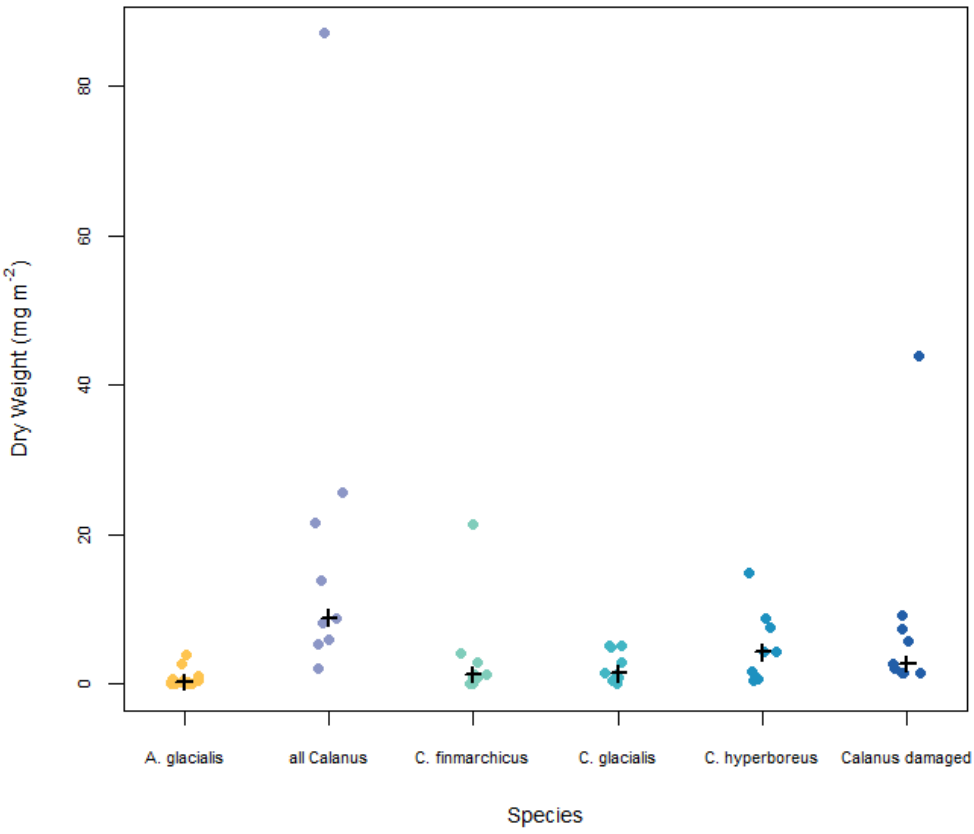

Fig. 3-6. Biomass in dry weight (mg m^{-2}) of each zooplankton species per Station. Median values of each group are marked in black. Biomasses of *C. hyperboreus*, *C. finmarchicus* and *C. glacialis* based on stages CIV, CV and Females. The category "all *Calanus*" includes the biomasses of the three *Calanus* species as well

as copepodites and damaged individuals. Number of Stations: n(*Apherusa*)=16, n(*Calanus*)=9 (excluding 73-7).

The sea ice at 12 of the 16 stations (station 63-1 to 75-6) consisted of first-year ice (FYI) and originated from the Central Arctic Ocean (CAO). At station 50-5, the only station located directly on the Barents Sea Shelf, the sea ice originated from the Laptev Sea and was 2 years old (second-year ice or multiyear-ice, MYI). The sea ice at the three stations close to Yermak Plateau (77-2, 78-5 and 79-1) consisted of 3 year-old MYI from the East Siberian Sea (ESS) (T. Krumpen, unpublished data).

Since three sea ice origin sectors were distinguishable, it seemed appropriate to take a closer look at the impact of ice origin on biomass values. The minima, maxima, median values and total biomasses of each zooplankton species per sea ice origin sectors were depicted in Table 2. It should be kept in mind that the number of stations was higher for CAO than ESS and therefore the results of ESS are more imprecise. Since copepod abundances were very high at station 78-5 (ESS) compared to all other stages, the total biomass of ESS stations was considerably higher than of CAO stations for *C. finmarchicus* and all *Calanus*, despite the lower number of stations.

Table 2. Biomass values of each species/group per sea ice origin sector

Species	Sea ice origin	Dry Weight (mg m^{-2})			n (Stations)
		Min	Median	Max	
A.glacialis	Laptev Sea	0.225	0.225	0.225	1
A.glacialis	Central Arctic Ocean	0.000	0.509	3.895	12
A.glacialis	East Siberian Sea	0.000	0.227	0.294	3
C. hyperboreus	Central Arctic Ocean	0.393	2.671	8.893	6
C. hyperboreus	East Siberian Sea	1.614	4.248	14.870	3
C. glacialis	Central Arctic Ocean	0.089	1.355	5.203	6
C. glacialis	East Siberian Sea	0.408	2.995	5.250	3
C. finmarchicus	Central Arctic Ocean	0.078	1.215	2.897	6
C. finmarchicus	East Siberian Sea	0.080	4.222	21.393	3
all *Calanus**	Central Arctic Ocean	2.033	7.065	25.691	6
all *Calanus**	East Siberian Sea	8.904	13.888	87.072	3

* includes biomasses of all *Calanus* species, copepodites and damaged individuals

Since *A. glacialis* was sampled at all of the 16 stations, the dry weights (mg m^{-2}) of this species were plotted as seen in Fig. 3-7 to show the different trends in biomass per sea ice origin sector. The CAO median value of 0.5 mg m^{-2} was only slightly higher than the ESS median value of 0.23 mg m^{-2}, since

data points of both sectors mainly gathered in the y-axis intercept between 0 and 1 mg m^{-2}. The dry weight value of the only station with sea ice that originated from Laptev Sea (50-5) was 0.225 mg m^{-2} and therefore lower than the median values of the other two sectors. While the maximum value of ESS stations constituted 0.29 mg m^{-2}, the dry weight measurements of CAO stations extended up to 3.89 mg m^{-2} when looking at outliers in the CAO data. The potential dry weight of samples caught below sea ice that originated in the CAO could therefore be estimated to reach considerably higher values compared to ESS stations.

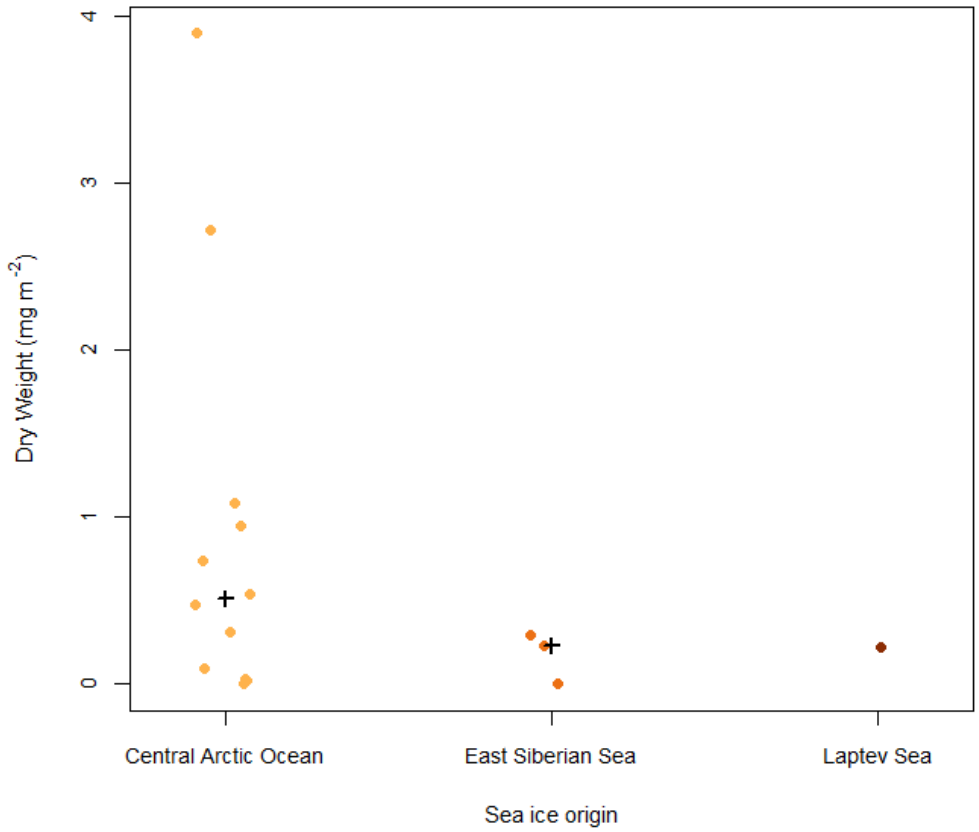

Fig. 3-7. Biomass in dry weight (mg m^{-2}) of *Apherusa glacialis*, split in the main sea ice origin sectors. Median values of Central Arctic Ocean and East Siberian Sea are marked in black. Data of 16 stations in the sampling area.

Based on the assumed patterns found in the distribution of biomasses, the influences of sea ice origin on dry weights (mg m^{-2}) of *A. glacialis* were tested for statistical significance with a Mann-Whitney-U-Test. No statistically significant correlation was found (W = 27.5, p-value = 0.1935). The influence

of water mass inflow on dry weights (mg m^{-2}) of *A. glacialis* was tested with the same method and showed even lower significance levels (W = 36.5, p-value = 0.6336).

4.4 Bulk Stable Isotope Analysis (BSIA)

All bulk stable carbon (δ $^{13}C/^{12}C$ (‰)) and nitrogen (δ $^{15}N/^{14}N$ (‰)) isotope values for each individual of both *Apherusa glacialis* and *Calanus* spp. were visualized in Fig. 3-8 shown below. Bulk stable nitrogen (δ ^{15}N) isotope values of *A. glacialis* ranged from 2.69 to 5.54 ‰ and were therefore overall lower than the nitrogen isotope values of *Calanus* spp., ranging from 5.35 to 8.27 ‰. Bulk stable carbon (δ ^{13}C) isotope values of *A. glacialis* ranged from -25.75 to -20.69 ‰ and were therefore higher than the carbon isotope values of *Calanus* spp., ranging from -28.47 to -26.10 ‰. Regarding station means within the species *A. glacialis*, two clusters of stations with the lowest nitrogen and medium carbon isotope values (70-1, 71-5, 73-7, 75-6) located in the Nansen Basin and stations with medium nitrogen and high carbon isotope values (50-5, 63-2, 65-4, 67-5, 78-5), located at or close to Barents Sea Shelf and slope were recognizable. Based on the location of the stations in the two clusters, the influence of water mass inflow on stable isotope content was tested for statistical significance with a Mann-Whitney-U-Test. Both stable δ ^{13}C (W = 99, p-value = 0.0001867) and stable δ ^{15}N isotope values (W = 101, p-value = 6.88e-05) showed a statistically significant correlation.

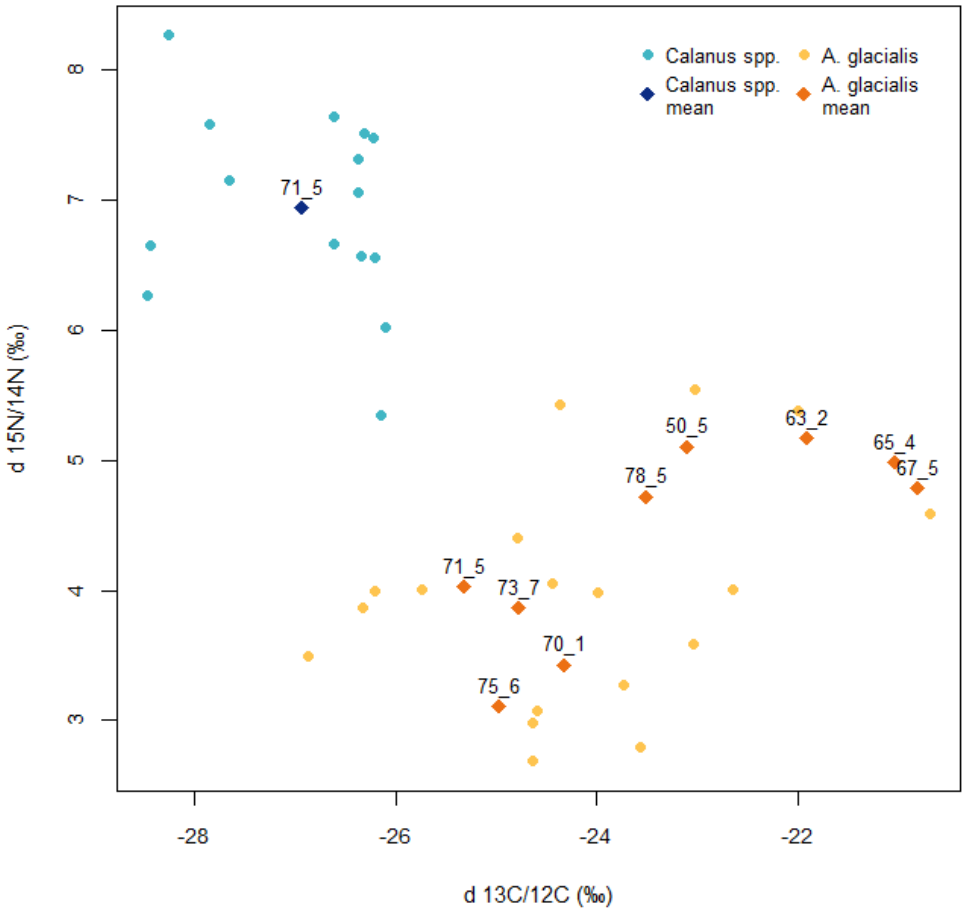

Fig. 3-8. Isotope measurements of δ $^{13}C/^{12}C$ (‰) and δ $^{15}N/^{14}N$ (‰). *Apherusa glacialis* (yellow/orange) and *Calanus* spp. (turquoise/blue) data are illustrated as values for each individual (points) and mean values per station (rhombs). Station numbers are plotted above the means.

4.5 Stomach content analysis (*Boreogadus saida*)

Stomach contents of the five dissected polar cod are shown in Table 3 below. Heavily digested stomach contents were hardly identifiable. Krill (*Thysanoessa* spp.) and Krill eyes seem to have withstood the digestive processes for the longest amount of time, presumably because of body size and material properties. *Thysanoessa inermis* was the most abundant Krill species. Stomach contents in better condition, found at station 50-5 and 70-1, showed comparatively high abundances in *Calanus* adult females (AF).

Station 50-5 was located on the shelf, station 67-5 on the shelf slope into the basin and station 70-1 directly in the Nansen Basin. The three polar cod

caught in the slope area show very low to zero abundance of calanoid copepods and the highest abundances in Krill. Furthermore, Amphipods were found in these three specimen, while none were found in the fish caught in shelf or basin area.

Table 3. Polar cod stomach contents (abundance in individuals)

Station		50-5	67-5	67-5	67-5	70-1
Degree of digestion		2	4	4	3	3
Calanus spp.	F	91	0	1	1	332
stages	CV	0	0	0	0	3
Copepods unidentified		0	0	0	1	31
A. glacialis		0	1	0	3	0
Amphipod unidentified		0	0	1	0	0
Thyssanoessa spp.		2	5	3	1	0
Krill eyes		12	16	6	0	0
Parasites		2	0	1	0	0

5 Discussion

5.1 Possible explanations of spatial variability

The study region was characterized by strong gradients in bathymetry and, stretching over almost 500 km in latidudinal extent, and extended over various hydrographical regimes (Flores and Macke, 2018; Heuzé *et al.*, 2018). During springtime 2017, the area was entirely covered by sea ice (as shown in Fig. 2-2), and significant melting only started in the southernmost area (station 50-5) and towards the end of expedition PS106. Hence, patterns in spatial variability of abundance, biomass and stable isotope content were probably driven by oceanographic features of the Arctic Ocean (AO), or by the variability of sea-ice properties in the observed area (David *et al.*, 2015; Flores *et al.*, 2019).

There are two gateways for Atlantic Water (AW) to flow into the Arctic, located to the West and East of Spitsbergen. Through the deep Fram Strait Branch (FSB) (sill depth ~2600 m) between Greenland and Spitsbergen, warm and salty Atlantic deep water can enter the Nansen Basin via the Yermak Plateau and flow northwards along the Eurasian shelf slope, until it reaches the slope of the Laptev Sea into the Amundsen Basin. The Barents Sea Opening between Spitsbergen and the Norwegian mainland functions as an inflow gateway for cooler and fresher AW that proceeds southward over the relatively shallow Barents Sea Shelf (sill depth ~400 m) and through the Kara Sea (Rudels, 2012; Bluhm, Kosobokova and Carmack, 2015).

Surface water in the northern Amundsen Basin (Polar Surface Water, PSW) flows southward as part of the cyclonic Trans-Polar Drift, one of the main circulatory systems in the AO. It is via this system that sea ice is transported from the Siberian Shelf passing the Central Arctic Ocean and exiting the Eurasian Basin through Fram Strait into the Nordic Seas (Kwok and Rothrock, 1999; Bluhm, Kosobokova and Carmack, 2015). The study area covered both the Atlantic inflow along the Eurasian shelf slope with stations near the shelf slope and near the Yermak Plateau (stations 50-5 to 68-5 and 77-2, 78-5, 79-1), and the PSW advected with the Transpolar Drift, which influenced the stations in the inner Nansen Basin (stations 69-2 to 75-6) (Nikolopoulos *et al.*, 2018). During expedition PS106/2, the sea ice at the three stations close to the Yermak Plateau (77-2, 78-5, 79-1) originated from the East Siberian Sea (ESS), and sea ice at one station on the Barents Sea Shelf (50-5) originated from the Laptev Sea shelf. According to the sea-ice

backtracking, this sea ice from the Siberian shelves was multiyear ice (ice age of 3 and 2 years). The majority of the sea ice in the Eastern part of the study area originated in the Central Arctic Ocean (CAO), and was classified as first-year ice (T. Krumpen, AWI, unpublished data).

The observed abundances of *Apherusa glacialis* (from zero or 0.01 ind. m^{-2} to 2.05 ind. m^{-2}) in this study were within the range previously reported from quantitative under-ice sampling. For example, (David *et al.*, 2015) reported a range from 0.05 to around 2 individuals per m^2 in the Nansen Basin during late summer, whereas (Schaafsma, 2018) reported lower values near the Yermak Plateau during springtime (mean abundance of 0.04 ind. m^{-2}). These studies were conducted with SUITs and can therefore be well compared to the present investigation. Other studies reported much lower and higher values based on sampling by e.g. SCUBA divers, pelagic nets or video recordings, but are difficult to compare to this dataset (Poltermann, 2001; Werner and Gradinger, 2002; Berge *et al.*, 2012).

At stations in the Eastern part of the study area at the slope from the Barents Sea shelf into the Nansen Basin (stations 63-1 to 69-2), abundances of *Apherusa glacialis* ranged between 0.16 ind. m^{-2} and reached a maximum of 2.05 ind. m^{-2}. In contrast, at stations close to the Yermak Plateau and on the shelf (50-5, 77-2, 78-5, 79-1), abundances of *A. glacialis* were ranging from zero to 0.15 ind. m^{-2}. This pattern could indicate that first-year ice floes from CAO supported higher abundances of the ice amphipod than multiyear ice from the Siberian shelves. Since new sea ice only forms in waters with a sufficiently low temperature, it is possible that the newly formed ice provided a cooler and therefore more preferable environment for *A. glacialis* to settle and reproduce in, while older sea ice might have undergone one or more melt cycles during drifting, during which ice amphipods could have left the under-ice habitat (Berge *et al.*, 2012). Older sea ice also has a higher chance of bearing a thicker snow cover limiting the amount of light available under the ice, which is an important factor for the growth of under-ice algae and therefore food availability for *A. glacialis*. Nevertheless, it should be kept in mind that at the Northern Nansen Basin stations (70-1 to 75-6) with sea ice from the CAO, abundances were generally lower than at the other Eastern Stations, ranging from zero to 0.5 ind. m^{-2}. It was suggested in

(Beuchel and Lønne, 2002) that population structures of *A. glacialis* were more affected by sea ice conditions than by the ice age itself.
For a complete picture of the distribution of a species though, abundances alone are insufficient. A high abundance of small juvenile individuals at one station might outweigh an adult-dominated population at another station in pure numbers, yet does not provide information on which station constitutes the more suitable habitat for zooplankton or better hunting ground for predators. Incorporating the density of biomass per station can be a more representative measure regarding the attractiveness of a habitat for a predator. Considering that predators can save energy when hunting for less prey with a higher energetic content, it would make sense that an area of lower abundance can still be a more favorable hunting ground when it provides a higher biomass and larger prey. Furthermore, a higher zooplankton biomass often indicates sufficient and high-quality food resources for animals to develop not only in high numbers but also to an optimal adult size.

In this study, biomass results, too, seemed to support the assumption that sea-ice origin was a driving influence behind the distribution of *A. glacialis*, as data showed distinct differences in the maxima of available biomass per sector, and median values showed a slight difference as well. But when tested for statistical significance with a Mann-Whitney-U-Test, no significant effect of sea ice origin on biomass could be detected. The inability to detect significant patterns in the biomass distribution were probably owed to the low sample size, especially of stations with sea ice originating from the East Siberian Sea, indicating that a larger sample size could have improved the robustness of the applied statistical test.

Another pattern considering spatial distribution comes to mind when looking at the results of bulk stable isotope analysis (BSIA). BSIA can be used as a tool to determine both the origin of food resources of a species and its trophic level, helping to better understand its role in the food-web (Peterson and Fry, 1987; Tamelander *et al.*, 2006; Newsome, Clementz and Koch, 2010).

The isotopic fingerprint of ice-originated carbon is characterized by a high proportion of stable δ 13 carbon isotopes. It is assumed that this is caused by sympagic systems like under-ice habitats being isolated from outside carbon influx (Peterson and Fry, 1987; Hecky and Hesslein, 1995). This can lead to carbon limitation as ice algae grow, enhancing the uptake of ^{13}C by

microalgae (Søreide *et al.*, 2013). The higher the stable δ ^{13}C content in a sample, the more likely it is that the observed species covers its carbon demand from ice-associated algae. Low δ ^{13}C contents indicate that the species covers its carbon demand mainly from pelagic phytoplankton.

The proportion of stable δ ^{15}N isotopes allows conclusions on the trophic level of the observed species. The higher the species ranks in the food-web, the higher the detected content in stable δ ^{15}N nitrogen. (reviewed by (Newsome, Clementz and Koch, 2010)) The content of stable δ ^{15}N isotopes in herbivorous species such as *A. glacialis* is therefore relatively low compared to omnivores and herbivores.

Both stable δ ^{13}C and δ ^{15}N isotope results for *A. glacialis* in this study align with the results of previous papers in this area. (Kohlbach *et al.*, 2016) detected a mean δ ^{13}C value of -22.3 ‰ in the Central Arctic Ocean during summertime, which lays in the range between -20.7 to -26.8 ‰ of this study. Compared to the mean value of 5.4 ‰ for δ ^{15}N reported by (Kohlbach *et al.*, 2016), many values in this study (range 2.69 to 5.5 ‰) were lower.

The wide range of δ ^{15}N values observed in this study reflected a distinct spatial pattern in stable isotope fractionations. The two observed clusters described in section 4.4 indicate regional differences in trophic carbon flux. Very low δ ^{15}N values at stations 70-1 to 75-6 may reflect an unusually low trophic baseline, as has been observed in this region during springtime by (Søreide *et al.*, 2006). The variability in δ ^{15}N values could further be attributed to the different oceanographic regimes in the study region, i.e. nutrient rich Atlantic inflow and more light availability (in spring) near the Barents/Svalbard shelf and the Yermak Plateau (Stations 50-5, 63-2, 67-5, 78-5) in contrast with nutrient-poor waters and lower light availability at the stations deeper in the Nansen Basin associated with lower d15N values (stations 70-1 to 75-6). When tested for statistical significance with a Mann-Whitney-U-Test, the suspected effect of water masses on the value of both stable δ ^{15}N and δ ^{13}C isotopes of *A. glacialis* in this study was supported. The reduced δ ^{13}C value at the northern stations in the Nansen Basin points to less carbon limitation in this region. This indicates that ice algal growth and therefore uptake of carbon did not yet rise to a level causing carbon limitation in the brine channels due to light limitation by a closed, snow-covered ice pack.

Distributional patterns of *Calanus* spp. were not tested, neither concerning biomass results nor stable isotope content, since the examined stations

were not evenly distributed across the sampling area. Comparing the mean biomass values of *Calanus* spp. per sea ice origin sector to the values of *A. glacialis*, the results for ice originating from the Central Arctic Ocean versus the East Siberian Sea showed a reversed pattern. Median dry weights of *Calanus* spp. were explicitly higher at stations with sea ice that originated from the East Siberian Sea (77-2, 78-5, 79-1), mainly because of the particularly high biomasses and abundances found at station 78-5. As described in (Zakharova, 2019), station 78-5 was located close to areas where phytoplankton blooms were observed. The high values found at station 78-5 could therefore be explained by an already occurred phytoplankton bloom, catalyzing the growth of zooplankton. Since *Calanus* spp. nourish themselves omnivorously on P-POM and smaller zooplankton species, the differences in d15N values to *A. glacialis* can be assumed to be based on a more omnivorous diet in *Calanus* spp..

The number of individuals per m^2 per station in the Nansen Basin reported by (David *et al.*, 2015) was much lower than in the present study, ranging from 0 to 31 ind. m^{-2} per station for all of the three *Calanus* species combined. This could be explained by seasonal changes in the distribution of *Calanus* spp., since samples of the previous study were collected in late summer during August and September.

An observation supporting the influence of Atlantic Water inflow on the shelf and slope stations was found regarding the species proportion of *C. finmarchicus* and *C. glacialis* at each station. Stages CIV and CV of the Atlantic species *C. finmarchicus* were predominant at the majority of stations. Higher proportions of females, however, were only found at the four examined stations close to the shelf (63-1, 65-4, 78-5, 79-1), where the main inflow of Atlantic Water prevails. As reviewed in (Bluhm, Kosobokova and Carmack, 2015), numerous papers have shown evidence that huge numbers of Atlantic expatriates like *C. finmarchicus* get advected into the Central Arctic Ocean every year and make up a majority of zooplankton biomass in the Eurasian Basin. At the examined northern stations in the Nansen Basin (71-5 to 75-6) influenced by Polar Surface Water, however, female individuals of Arctic species *C. glacialis* clearly dominated. Abundances of the Arctic species *C. hyperboreus* were also the highest in this region.

As a main contrast between abundances and biomasses of *Calanus* spp. and *A. glacialis* it can be stated that the results of *Calanus* spp. align with

the occurrence of water bodies, while the results of *A. glacialis* match the origins of sea ice. Regarding the differences in stable isotope contents, the results of this study align with common knowledge about food-webs in marine sympagic ecosystems (Bradstreet and Cross, 1982; Søreide *et al.*, 2006). While only one station of *Calanus* spp. was taken into account for BSIA, the mean values of $\delta\ ^{15}N$ and $\delta\ ^{13}C$ supported the findings made in previous studies. Comparing the results of *Calanus* spp. to the detected values for *C. glacialis* in (Kohlbach *et al.*, 2016), the ranges from -26.1 to -28.5 ‰ for $\delta\ ^{13}C$ and 5.4 to 8.3 ‰ for $\delta\ ^{15}N$ found in this study are in line with the reported mean δ 13C values of -26.8 ‰ and mean $\delta\ ^{15}N$ values of 7.5 ‰. As *Calanus* spp. was shown to practice a more omnivorous diet than *A. glacialis*, stable $\delta\ ^{15}N$ isotope values were expectably higher, signaling a higher trophic level of the species. Lower content of $\delta\ ^{13}C$ on the other hand indicated that *Calanus* spp. fed less on ice algae than the ice-associated species *A. glacialis* (Kohlbach *et al.*, 2016).

In spite of their dominance in abundance and biomass throughout the research area, *Calanus* spp. or other copepods were only found in larger numbers in the diet of the examined specimens of *Boreogadus saida* in the samples from shelf (50-5) and basin (70-1) area. In samples from the slope (67-5), mostly euphausiids were detected, which were abundant within the upper 100 m (Zakharova, 2019). Amphipods were only detected in the slope station samples. The findings of this study are contrasting the results of (Kohlbach, Schaafsma, *et al.*, 2017) reporting a polar cod diet that heavily relies on sympagic species like *A. glacialis*.

5.2 Conclusions

Based on the findings of this study, it is challenging to asses which of the examined stations would offer the most attractive under-ice habitat for polar cod. Combining the results of *A. glacialis* and *Calanus* spp., it appears that the stations located in the Nansen Basin would present a most favorable hunting ground. Especially the most northern stations with sea ice from the Central Arctic Ocean which were influenced by Polar Surface Water would provide predators with the highest abundances of *Calanus hyperboreus*, the largest copepod species containing the highest amount of nutritious lipids. Abundances of *Apherusa glacialis* on the other hand were highest closer to the Barents Shelf slope, where copepod abundances were not investigated. With more data becoming available, the Barents Sea shelf slope could thus be confirmed to host the best foraging ground for polar cod in the under-ice habitat.

Regarding hypothesis a) described in 2.7, distinct spatial variabilities were shown, but could only be traced back to water masses. Connections between spatial variability and depth levels or ice origin in the examined area were suggested. In regards to hypothesis b), variabilities in the food resources of *B. saida* were shown, but no direct correlation between detected zooplankton distributions at the different locations and the proportion of species in stomach contents was suggested.

As climate change will continue to drastically alter sea ice conditions and oceanographic properties in polar regions, huge shifts in the availability and properties of under-ice habitats and their communities are expected to occur. The results of this study demonstrate that the rapid transformation of Arctic ecosystems may affect the distribution of their inhabitants and the transfer of energy and carbon in Arctic food-webs.

6 Acknowledgements

First and foremost, I would like to thank my supervisor Dr. Hauke Flores for his great support, patience, humor and for giving me the opportunity to write my thesis at AWI. Furthermore, I would like to thank Dr. Fokje Schaafsma for taking the time to supervise me at WMR and for taking me on a test drive with the new research speed boat. I would like to thank Prof. Dr. Ralph Tollrian for supervising me at RUB, reviewing my thesis and helping me with all of my questions.

Thank you to Dr. Nicole Hildebrandt, Dr. Astrid Cornils and Dr. Barbara Niehoff from PolBiolOz, who provided me with plenty of information on everything copepod-related. Thank you to Nadine Knüppel for counting amphipods and to Sandra Murawski, who helped me out numerous times with the freezedrier, the preparation of isotope samples and when the scales were acting crazy during the summer heat-waves.

I am grateful to have made many friends in Bremerhaven and the Netherlands during this time. Especially Lora Strack van Schijndel, Tobias Strickmann, Nadezhda Zakharova, Josefine Weiss and Annette Albrecht were incredibly supportive on a personal as well as professional level. I also want to thank all my couchsurfing hosts for letting me crash at their places. I could not have written this thesis without the emotional support of Markus Böddeker, Julia Beukert, Laura Klasmeier and of course Charlotte Herz (without which I probably never would have submitted my application for AWI in the first place).

Finally, a big thank you goes out to all the kind souls who actively participate in Stackoverflow R Help forums. You have made my life a whole lot easier.

Sea ice concentration data from 2019-09-08 and from 2017-07-20 to 2017-06-23 were obtained from http://www.meereisportal.de (grant: REKLIM-2013-04).

7 Appendix

7.1 Supplementary material

Table 4. Species proportion in *Calanus* spp. length measurements

Station	Stage	*Calanus finmarchicus*	*Calanus glacialis*	Total	n
63-1	CIV	0.40	0.60	1	25
63-1	CV	0.89	0.11	1	19
63-1	F	0.67	0.33	1	9
65-4	CIV	0.50	0.50	1	2
65-4	CV	0.90	0.10	1	10
65-4	F	0.56	0.44	1	18
71-5	CIV	0.93	0.07	1	28
71-5	CV	0.90	0.10	1	94
71-5	F	0.37	0.63	1	94
72-5	CIV	0.97	0.03	1	73
72-5	CV	0.86	0.14	1	66
72-5	F	0.08	0.92	1	63
73-7	CIV	1.00	0.00	1	23
73-7	CV	0.58	0.42	1	26
73-7	F	0.02	0.98	1	55
74-5	CIV	0.74	0.26	1	23
74-5	CV	0.82	0.18	1	22
74-5	F	0.11	0.89	1	70
75-6	CIV	1.00	0.00	1	11
75-6	CV	0.91	0.09	1	57
75-6	F	0.41	0.59	1	56
77-2	F	0.00	1.00	1	10
78-5	CIV	0.94	0.06	1	65
78-5	CV	0.95	0.05	1	111
78-5	F	0.68	0.32	1	75
79-1	CIV	1.00	0.00	1	44
79-1	CV	0.97	0.03	1	76
79-1	F	0.82	0.18	1	33

Table 5. List of BSIA stations		
Station	**Species**	**n (Individuals)**
50-5	Apherusa glacialis	1
63-2	Apherusa glacialis	3
65-4	Apherusa glacialis	1
67-5	Apherusa glacialis	1
70-1	Apherusa glacialis	3
71-5	Apherusa glacialis	2
71-5	Calanus spp.	15
73-8	Apherusa glacialis	4
75-6	Apherusa glacialis	4
78-5	Apherusa glacialis	2

Table 6. Technical details of microscope and camera	
Material	**Model**
Program	Leica Application Suite (LAS) version 4.12.0
Microscope	Leica M205 C
Optics carrier	M205C 20, 5:1 zoom 0,78x-16,0x
Eyepiece	10x/23B
Tube	Ergotonic 100% Magnification 1
Camera adapter	0,5x
Main objective	0,63x
Brand	Leica Microsystems (Switzerland) Limited. Leica Microsystems CMS GmbH

7.2 Abbreviations

AO	Arctic Ocean
AW	Atlantic Water
BSIA	Bulk Stable Isotope Analysis
CAO	Central Arctic Ocean
ESS	East Siberian Sea
FYI	First-year ice
MYI	Multiyear ice
PLK	Zooplankton net
SUIT	Surface and Under-Ice Trawl
I-/P-POM	ice/pelagic particulate organic matter

8 List of figures and tables

8.1 Figures

8.2 Tables

9 Declaration of Authorship

ERKLÄRUNG

Hiermit erkläre ich an Eides statt, dass ich die heute eingereichte Bachelorarbeit selbständig verfasst und keine anderen als die angegebenen Quellen und Hilfsmittel benutzt sowie Zitate kenntlich gemacht habe. Bei der vorliegenden Bachelorarbeit handelt es sich um in Wort und Bild völlig übereinstimmende Exemplare.

Weiterhin erkläre ich, dass digitale Abbildungen als solche gekennzeichnet sind und nur die originalen Daten enthalten und in keinem Fall inhaltsverändernde Bildbearbeitung vorgenommen wurde.

Bochum, den

_____

Unterschrift

10 References

Ackley, S. F. and Sullivan, C. W. (1994) 'Physical controls on the development and characteristics of Antarctic sea ice biological communities— a review and synthesis', *Deep Sea Research Part I: Oceanographic Research Papers*. Pergamon, 41(10), pp. 1583–1604. doi: 10.1016/0967-0637(94)90062-0.

Arndt, C. E. and Swadling, K. M. (2006) 'Crustacea in Arctic and Antarctic Sea Ice: Distribution, Diet and Life History Strategies', in Southward, A. J. and Sims, D. W. (eds) *Advances in Marine Biology, Volume 51*. Elsevier Ltd, pp. 198–321. doi: 10.1192/bjp.112.483.211-a.

Arnkværn, G., Daase, M. and Eiane, K. (2005) 'Dynamics of coexisting Calanus finmarchicus, Calanus glacialis and Calanus hyperboreus populations in a high-Arctic fjord', *Polar Biology*, 28(7), pp. 528–538. doi: 10.1007/s00300-005-0715-8.

Ashjian, C. J. *et al.* (2003) 'Annual cycle in abundance, distribution, and size in relation to hydrography of important copepod species in the western Arctic Ocean', *Deep-Sea Research Part I: Oceanographic Research Papers*, 50(10–11), pp. 1235–1261. doi: 10.1016/S0967-0637(03)00129-8.

Berge, J. *et al.* (2012) 'Retention of ice-associated amphipods: Possible consequences for an ice-free Arctic Ocean', *Biology Letters*, 8(6), pp. 1012–1015. doi: 10.1098/rsbl.2012.0517.

Beuchel, F. and Lønne, O. J. (2002) 'Population dynamics of the sympagic amphipods Gammarus wilkitzkii and Apherusa glacialis in sea ice north of Svalbard', *Polar Biology*, 25(4), pp. 241–250. doi: 10.1007/s00300-001-0329-8.

Bluhm, B. A., Kosobokova, K. N. and Carmack, E. C. (2015) 'A tale of two basins: An integrated physical and biological perspective of the deep Arctic Ocean', *Progress in Oceanography*. Elsevier Ltd, 139(August), pp. 89–121. doi: 10.1016/j.pocean.2015.07.011.

Bradstreet, M. S. W. and Cross, W. E. (1982) 'Trophic Relationships at High Arctic Ice Edges', *Arctic*, 35(1), pp. 1–12. doi: 10.14430/arctic2303.

Choquet, M. *et al.* (2017) 'Genetics redraws pelagic biogeography of Calanus', *Biology Letters*, 13(12), p. 20170588. doi: 10.1098/rsbl.2017.0588.

Christiansen, J. S. *et al.* (2012) 'Trophic ecology of sympatric Arctic gadoids, Arctogadus glacialis (Peters, 1872) and Boreogadus saida (Lepechin, 1774), in NE Greenland', *Polar Biology*, 35(8), pp. 1247–1257. doi: 10.1007/s00300-012-1170-y.

Comiso, J. C. (2003) 'Warming trends in the Arctic from clear sky satellite observations', *Journal of Climate*, 16(21), pp. 3498–3510. doi: 10.1175/1520-0442(2003)016<3498:WTITAF>2.0.CO;2.

Conover, R. J. (1988) 'Comparative life histories in the genera *Calanus* and *Neocalanus* in high latitudes of the northern hemisphere', *Hydrobiologia*, 167–168(1), pp. 127–142. doi: 10.1007/BF00026299.

Cottier, F., Steele, M. and Nilsen, F. (2017) 'Sea ice and Arctic Ocean oceanography', in Thomas, D. N. (ed.) *Sea Ice*. John Wiley & Sons, Ltd., pp. 197–215.

Daase, M. *et al.* (2018) 'New insights into the biology of Calanus spp. (Copepoda) males in the Arctic', *Marine Ecology Progress Series*, 607, pp. 53–69.

David, C. *et al.* (2015) 'Community structure of under-ice fauna in the Eurasian central Arctic Ocean in relation to environmental properties of sea-ice habitats', *Marine Ecology Progress Series*, 522, pp. 15–32. doi: 10.3354/meps11156.

David, C. *et al.* (2016) 'Under-ice distribution of polar cod Boreogadus saida in the central Arctic Ocean and their association with sea-ice habitat properties', *Polar Biology*. Springer Berlin Heidelberg, 39(6), pp. 981–994. doi: 10.1007/s00300-015-1774-0.

Falk-Petersen, S. *et al.* (2009) 'Lipids and life strategy of Arctic Calanus', *Marine Biology Research*, 5(1), pp. 18–39. doi: 10.1080/17451000802512267.

Flores, H. *et al.* (2012) 'The association of Antarctic krill Euphausia superba with the under-ice habitat', *PLoS ONE*, 7(2). doi: 10.1371/journal.pone.0031775.

Flores, H. *et al.* (2019) 'Sea - ice properties and nutrient concentration as drivers of the taxonomic and trophic structure of high - Arctic protist and metazoan communities', *Polar Biology*. Springer Berlin Heidelberg, (0123456789). doi: 10.1007/s00300-019-02526-z.

Flores, H. and Macke, A. (2018) *The Expeditions PS106/1 and 2 of the Research Vessel POLARSTERN to the Arctic Ocean in 2017, Berichte zur Polar- und Meeresforschung*. doi: 10.2312/BzPM_0714_2017.

Franeker, J. A. Van, Flores, H. and Dorssen, M. Van (2009) 'The Surface and Under-Ice Traw l (SUIT)', (January 2012), pp. 1–5.

Grosfeld, K. *et al.* (2016) *Online sea-ice knowledge and data platform <www.meereisportal.de>, 85 (2)*. doi: doi:10.2312/polfor.2016.011.

Gulliksen, B. and Lønne, O. J. (1989) 'Distribution, abundance, and ecological importance of marine sympagic fauna in the Arctic', *Zooplankton and sea-ice fauna Rapp.*, 188, pp. 133–138. Available at: https://www.researchgate.net/publication/271204236.

Hecky, R. . and Hesslein, R. H. (1995) 'Contributions of Benthic Algae to Lake Food Webs as Revealed by Stable Isotope Analysis Author (s): R . E . Hecky and R . H . Hesslein Source : Journal of the North American Benthological Society , Vol . 14 , No . 4 (Dec ., 1995), Published by : The U', *North American Benthological Society*, 14(4), pp. 631–653.

Heuzé, C. *et al.* (2018) *Physical oceanography during POLARSTERN cruise PS106/2 (ARK-XXXI/1.2)*. doi: https://doi.org/10.1594/PANGAEA.885443.

Hirche, H. *et al.* (1994) 'The Northeast Water polynya, Greenland Sea - III. Meso- and macrozooplankton distribution and production of dominant

herbivorous copepods during spring', *Polar Biology*, 14(7), pp. 491–503. doi: 10.1007/BF00239054.

Hirche, H. J. and Kwasniewski, S. (1997) 'Distribution, reproduction and development of Calanus species in the Northeast Water in relation to environmental conditions', *Journal of Marine Systems*. doi: 10.1016/S0924-7963(96)00057-7.

Hop, H. and Gjøsæter, H. (2013) 'Polar cod (Boreogadus saida) and capelin (Mallotus villosus) as key species in marine food webs of the Arctic and the Barents Sea', *Marine Biology Research*, 9(9), pp. 878–894. doi: 10.1080/17451000.2013.775458.

Klekowski, R. Z. and Weslawski, J. M. (1991) *Atlas of the Marine Fauna of Southern Spitzbergen, Vol.2 Invertebrates Part 1.* Gdansk, Poland: Institute of Oceanology, Polish Academy of Sciences.

Kock, K. H. *et al.* (2008) 'The biology of the spiny icefish Chaenodraco wilsoni Regan, 1914', *Polar Biology*, 31(3), pp. 381–393. doi: 10.1007/s00300-007-0366-z.

Kohlbach, D. *et al.* (2016) 'The importance of ice algae-produced carbon in the central Arctic Ocean ecosystem: Food web relationships revealed by lipid and stable isotope analyses', *Limnology and Oceanography*, 61(6), pp. 2027–2044. doi: 10.1002/lno.10351.

Kohlbach, D., Lange, B. A., *et al.* (2017) 'Ice Algae-Produced Carbon Is Critical for Overwintering of Antarctic Krill Euphausia superba', *Frontiers in Marine Science*, 4(September), pp. 1–16. doi: 10.3389/fmars.2017.00310.

Kohlbach, D., Schaafsma, F. L., *et al.* (2017) 'Strong linkage of polar cod (Boreogadus saida) to sea ice algae-produced carbon: Evidence from stomach content, fatty acid and stable isotope analyses', *Progress in Oceanography*. Elsevier Ltd, 152, pp. 62–74. doi: 10.1016/j.pocean.2017.02.003.

Kohlbach, D. *et al.* (2018) 'Dependency of Antarctic zooplankton species on ice algae-produced carbon suggests a sea ice-driven pelagic ecosystem during winter', *Global Change Biology*, 24(10), pp. 4667–4681. doi: 10.1111/gcb.14392.

Kosobokova, K. (1999) 'The reproductive cycle and life history of the Arctic copepod Calanus glacialis in the White Sea', *Polar Biology*, 22(4), pp. 254–263. doi: 10.1007/s003000050418.

Kosobokova, K. and Hirche, H.-J. (2009) 'Biomass of zooplankton in the eastern Arctic Ocean - a base line study', *Progress in Oceanography*, 82(4), pp. 265–280. doi: 10.1016/j.pocean.2009.07.006.

Kwasniewski, S. *et al.* (2003) 'Distribution of calanus species in Kongsfjorden', *Journal of Plankton Research*, 25, pp. 1–20.

Kwok, R. and Rothrock, D. A. (1999) 'Variability of Fram Strait ice flux temperature 2 , -7 % of the area of the Arctic Ocean . The winter area flux ranges from a minimum to a maximum of October May 1995 is 1745 km from a low of 1375 km the 1990 flux to a high of 2791 km The sea level pressu', *Journal*

of Geophysical Research, 104(1998), pp. 5177–5189.

LIENs Stable Isotope Facility (2014) 'Appendix 2: Sample preparation protocols'. LIENs SIF. Available at: https://lienss.univ-larochelle.fr/IMG/pdf/lienss_sif_appendix_2_protocols_v3-8.pdf.

Lønne, O. J. and Gulliksen, B. (1989) 'Size, age and diet of polar cod, Boreogadus saida (Lepechin 1773), in ice covered waters', *Polar Biology*, 9(3), pp. 187–191. doi: 10.1007/BF00297174.

Lubin, D. and Massom, R. (2006) *Polar Remote Sensing, Volume 1, Atmosphere and Oceans*. Springer Verlag, via https://www.meereisportal.de/de/meereisbeobachtung/beobachtungsgroessen/meereisbedeckung/, retrieved on 22 August 2019.

Motoda, S. (1959) 'Instructions for use devices of simple plankton apparatus Faculty of Fisheries , Hokkaido University', *Memoirs of the faculty of fisheries hokkaido university*, 7(1–2), pp. 73–111. Available at: http://hdl.handle.net/2115/21829.

Newsome, S. D., Clementz, M. T. and Koch, P. L. (2010) 'Using stable isotope biogeochemistry to study marine mammal ecology', *Marine Mammal Science*, 26(3), pp. 509–572. doi: 10.1111/j.1748-7692.2009.00354.x.

Nikolopoulos, A. *et al.* (2018) 'Physical Oceanography', in Flores, H. and Macke, A. (eds) *The Expeditions PS106/1 and 2 of the Research Vessel POLARSTERN to the Arctic Ocean in 2017*, pp. 60–72.

Perovich, D. K. (2011) 'The changing arctic sea ice cover', *Oceanography*, 24(3), pp. 162–173. doi: 10.5670/oceanog.2011.68.

Peterson, B. J. and Fry, B. (1987) 'Stable isotopes in ecosystem studies.', *Annual review of ecology and systematics. Vol. 18*, pp. 293–320.

Poltermann, M. (2001) 'Arctic sea ice as feeding ground for amphipods - Food sources and strategies', *Polar Biology*, 24(2), pp. 89–96. doi: 10.1007/s003000000177.

Poltermann, M., Hop, H. and Falk-Petersen, S. (2000) 'Life under Arctic sea ice - Reproduction strategies of two sympagic (ice-associated) amphipod species, Gammarus wilkitzkii and Apherusa glacialis', *Marine Biology*, 136(5), pp. 913–920. doi: 10.1007/s002270000307.

Richter, C. (1994) *Regional and seasonal variability in the vertical distribution of mesozooplankton in the Greenland Sea*, *PhD Thesis; Berichte zur Polarforschung*. Available at: http://epic.awi.de/26332/1/BerPolarforsch1994154.pdf.

Rudels, B. (2012) 'Arctic Ocean circulation and variability – Advection and external forcing encounter constraints and local processes', *Ocean Science*, 8(2), pp. 261–286. doi: 10.5194/os-8-261-2012.

Schaafsma, F. L. (2018) *Life in the polar oceans: the role of sea ice in the biology and ecology of marine species*. Wageningen University, Wageningen, the

Netherlands (2018).

Schlitzer, R. (2018) 'Ocean Data View'. Available at: http://odv.awi.de.

Søreide, J. E. *et al.* (2006) 'Seasonal food web structures and sympagic-pelagic coupling in the European Arctic revealed by stable isotopes and a two-source food web model', *Progress in Oceanography*, 71(1), pp. 59–87. doi: 10.1016/j.pocean.2006.06.001.

Søreide, J. E. *et al.* (2013) 'Sympagic-pelagic-benthic coupling in Arctic and Atlantic waters around Svalbard revealed by stable isotopic and fatty acid tracers', *Marine Biology Research*, 9(9), pp. 831–850. doi: 10.1080/17451000.2013.775457.

Spreen, G., Kaleschke, L. and Heygster, G. (2008) 'Sea ice remote sensing using AMSR-E 89 GHz channels', *J. Geophys. Res.*, 113(C02S03). doi: doi:10.1029/2005JC003384.

Tamelander, T. *et al.* (2006) 'Fractionation of stable isotopes in the Arctic marine copepod Calanus glacialis: Effects on the isotopic composition of marine particulate organic matter', *Journal of Experimental Marine Biology and Ecology*, 333(2), pp. 231–240. doi: 10.1016/j.jembe.2006.01.001.

Thomas, D. N. (2017) *Sea Ice*. 3rd edn. Chichester, UK ; Hoboken, NJ: John Wiley & Sons, Ltd.

Unstad, K. H. and Tande, K. S. (1991) 'Depth distribution of Calanus finmarchicus and C. glacialis in relation to environmental conditions in the Barents Sea', *Polar Research*, 10(2), pp. 409–420. doi: 10.1111/j.1751-8369.1991.tb00662.x.

Vaughan, D. G. *et al.* (2013) 'Observations: Cryosphere', in Stocker, T. F. et al. (eds) *Climate Change 2013: The Physical Science Basis. Contribution of Working Group I to the Fifth Assessment Report of the Intergovernmental Panel on Climate Change*. AR5 edn. Cambridge University Press. doi: 10.1017/CBO9781107415324.Summary.

Wang, M. and Overland, J. E. (2009) 'A sea ice free summer Arctic within 30 years?', *Geophysical Research Letters*, 36(7), pp. 2–6. doi: 10.1029/2009GL037820.

Wang, M. and Overland, J. E. (2012) 'A sea ice free summer Arctic within 30 years: An update from CMIP5 models', *Geophysical Research Letters*, 39(17), pp. 6–11. doi: 10.1029/2012GL052868.

Werner, I. and Auel, H. (2005) 'Seasonal variability in abundance, respiration and lipid composition of Arctic under-ice amphipods', *Marine Ecology Progress Series*, 292, pp. 251–262. doi: 10.3354/meps292251.

Werner, I. and Gradinger, R. (2002) 'Under-ice amphipods in the Greenland Sea and Fram Strait (Arctic): Environmental controls and seasonal patterns below the pack ice', *Marine Biology*, 140(2), pp. 317–326. doi: 10.1007/s00227-001-0709-1.

Zakharova, N. (2019) *Trophic structure and biomass of high-Arctic zooplankton in the Eurasian Basin in 2017.* Saint Petersburg State University/Hamburg University.